Lecture Notes

Contact Mechanics and Elements of Tribology

Vladislav A. Yastrebov

CNRS, Mines Paris - PSL
CNRS UMR 7633, Centre des matériaux
Versailles, France

February 24-27, 2026

Copyright Notice

Abstract

These lecture notes cover the content of the course ″Contact Mechanics and Elements of Tribology″ that I taught for 11 years in the Master's program "Design of Materials and Structures" at the Centre des Matériaux of Mines Paris.

V.A. Yastrebov
Fontainebleau - Versailles - Paris

20 February 2026

Contents

Chapter 1

Continuum Contact Mechanics

1.1 Governing Equations of Elasticity

Boundary value problem in elasticity We consider a deformable body occupying a domain Ω in the reference configuration. A material point $\underline{X}$ is mapped to its current position $\underline{x}$ by the displacement field $\underline{u}$:

$$\underline{x} = \underline{X} + \underline{u}. \tag{1.1}$$

In the quasi-static regime, mechanical equilibrium (strong form) reads

$$\nabla \cdot \underline{\underline{\sigma}} + \rho \underline{f}_v = 0, \qquad \forall \underline{x} \in \Omega^i, \tag{1.2}$$

where $\underline{\underline{\sigma}}$ is the (Cauchy) stress tensor, ρ the mass density, and $\underline{f}_v$ the body force density. Here $\nabla(\cdot)$ denotes the spatial gradient/divergence (with respect to $\underline{x}$).

The infinitesimal strain tensor is defined from displacement compatibility as the symmetric part of the displacement gradient:

$$\underline{\underline{\varepsilon}} = \frac{1}{2}\left(\nabla \underline{u} + (\nabla \underline{u})^{\mathsf{T}}\right). \tag{1.3}$$

(In the slide notation, $\underline{u}\nabla$ is understood as $(\nabla \underline{u})^{\mathsf{T}}$.)

Assuming a (small-strain) hyperelastic constitutive law, the stress derives from a strain energy density $W(\underline{\underline{\varepsilon}})$:

$$\underline{\underline{\sigma}} = W'(\underline{\underline{\varepsilon}}). \tag{1.4}$$

The boundary is decomposed into disjoint parts Γ_u and Γ_f with $\partial\Omega = \Gamma_u \cup \Gamma_f$ and $\Gamma_u \cap \Gamma_f = \varnothing$. Dirichlet boundary conditions prescribe the displacement on Γ_u:

$$\underline{u} = \underline{u}^0, \qquad \forall \underline{x} \in \Gamma_u. \tag{1.5}$$

Neumann boundary conditions prescribe the traction on Γ_f:

$$\underline{\underline{\sigma}} \cdot \underline{n} = \underline{t}^0, \qquad \forall \underline{x} \in \Gamma_f, \tag{1.6}$$

where $\underline{n}$ is the outward unit normal.

Intuitive contact conditions Consider two deformable bodies occupying domains $\Omega^1(t)$ and $\Omega^2(t)$ in the current configuration (see Figure 1.1). The classical boundary value problem must be supplemented by additional conditions on the potential contact interface Γ_c^i.

We first state the intuitive conditions corresponding to frictionless and non-adhesive (or in other terms unilateral) contact. Their geometric meaning is illustrated in Figure 1.2.

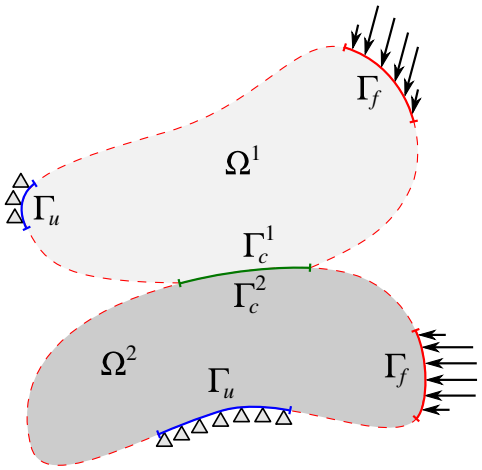

Figure 1.1: Two deformable bodies in contact.

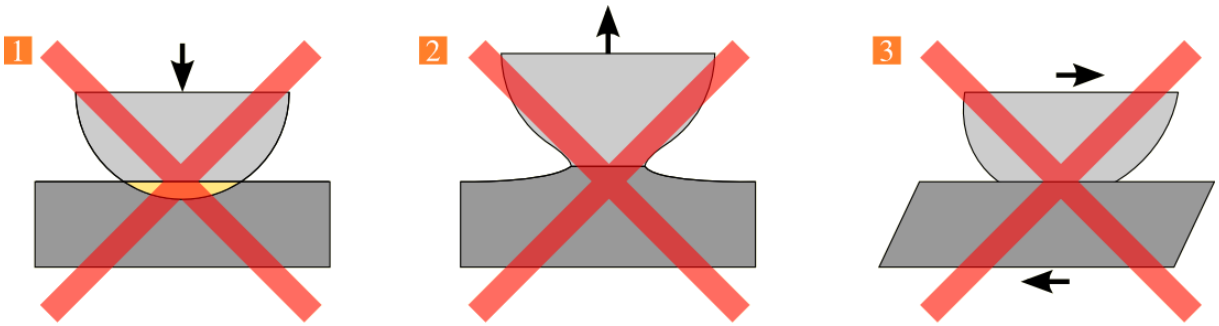

Figure 1.2: Intuitive representation of the contact conditions for frictionless and non-adhesive contact: no interpenetration, compressive normal stress only, and zero tangential traction.

1. No penetration The two bodies cannot interpenetrate. In the current configuration, their occupied domains must remain disjoint:

$$\Omega^1(t) \cap \Omega^2(t) = \emptyset. \tag{1.7}$$

2. No adhesion Contact can transmit compressive normal stresses only. Tensile normal tractions are not admissible, i.e. the normal component of the traction vector $\underline{t} = \underline{\underline{\sigma}} \cdot \underline{n}$ should be always non-negative[1]

$$\underline{n} \cdot \underline{\underline{\sigma}} \cdot \underline{n} = \underline{t} \cdot \underline{n} \leq 0, \qquad \forall \underline{x} \in \Gamma_c^i. \tag{1.8}$$

3. No shear stress (frictionless contact) In the absence of friction, the tangential component of the traction vector must vanish. This is expressed by projecting the stress tensor onto the tangential plane:

$$\underline{n} \cdot \underline{\underline{\sigma}} \cdot \left(\underline{\underline{I}} - \underline{n} \otimes \underline{n}\right) = \underline{t} \cdot \left(\underline{\underline{I}} - \underline{n} \otimes \underline{n}\right) = 0, \qquad \forall \underline{x} \in \Gamma_c^i. \tag{1.9}$$

The tensor $\underline{\underline{I}} - \underline{n} \otimes \underline{n}$ is the orthogonal projector onto the tangent plane.

[1] Of course, in case of interfacial fluid exerting pressure, this condition should be reconsidered.

1.2 Gap Function

Definition of the gap function The intuitive condition of non-penetration is not sufficient to properly formulate the contact problem, therefore it is reformulated in terms of a scalar *gap function* g, sometimes called *separation function*. This is the central kinematic quantity in contact mechanics and it governs the normal contact. It measures the signed distance between the two potential contact surfaces. Thus, penetration corresponds to a negative gap.

By convention:

$$\begin{cases} g > 0 & \text{separation,} \\ g = 0 & \text{contact,} \\ g < 0 & \text{penetration.} \end{cases} \tag{1.10}$$

In practice, to define the gap, we introduce a certain asymmetry in the problem discretization by assigning different roles to contacting surfaces. One surface will be called *slave surface* Γ_s and the gap will be defined for all points of this surface $\underline{\boldsymbol{r}}_s \in \Gamma_s$ with respect to the *master surface* Γ_m (see Figure 1.3).

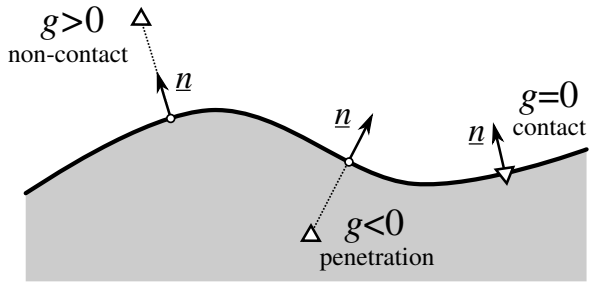

Figure 1.3: Gap between a slave point and a master surface.

1.2.1 Normal gap

If $\underline{\boldsymbol{r}}_s \in \Gamma_s$ denotes a slave point and $\underline{\boldsymbol{\rho}}(\xi)$ is a point on the master surface parametrized by parameter ξ. Let $\underline{\boldsymbol{n}}(\xi)$ be the associated unit outward normal on the master surface. Then we can define the *normal gap* as

$$g_n = \underline{\boldsymbol{n}} \cdot \left(\underline{\boldsymbol{r}}_s - \underline{\boldsymbol{\rho}}(\xi_\pi) \right), \tag{1.11}$$

where ξ_π is the coordinate of the master point, which is the closest to the slave node $\underline{\boldsymbol{r}}_s$. The problem of finding the closest point can be formulated as the following optimization problem:

$$\xi_\pi = \arg\min F(\underline{\boldsymbol{r}}_s, \xi), \quad F(\underline{\boldsymbol{r}}_s, \xi) = \tfrac{1}{2}(\underline{\boldsymbol{r}}_s - \rho(\xi))^2, \tag{1.12}$$

the solution of this problem for unbounded ξ corresponds to the stationary point with respect to variable ξ:

$$\frac{\partial F}{\partial \xi} = (\underline{\boldsymbol{r}}_s - \rho(\xi)) \cdot \frac{\partial \rho}{\partial \xi} = 0, \tag{1.13}$$

where $\partial\rho/\partial\xi = \tau$ is simply the tangent vector. So the problem of finding the closest point corresponds to finding a master point $\rho(\xi)$ at which the tangent vector is orthogonal to the vector connecting $\underline{\boldsymbol{r}}_s$ and $\rho(\xi)$. The geometric interpretation of the normal gap is illustrated in Figure 1.4.

Of course, to use Equations (1.12) and (1.13) we need to ensure that the tangent vector exists which implies that locally, the surface should be at least C^1 smooth, i.e. do not contain kinks and cusps. In the general case the closest-point projection can be defined as an infimum over different projections onto (i) smooth patches, (ii) line defects across which the normal is not continuos and (iii) point defects at which the normal cannot be defined (Yastrebov 2013; Aragón, Yastrebov, and Molinari 2013).

Using normal gap is not the only possibility to formulate the contact problem, but it presents a very natural choice.

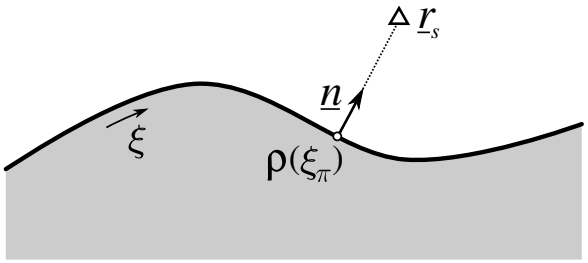

Figure 1.4: Definition of the normal gap as the projection of the slave-master distance onto the normal direction.

1.2.2 Frictionless (normal) contact conditions

Let us first introduce a short notation for the normal contact stress σ_n and the tangential traction vector as

$$\sigma_n = (\underline{\underline{\sigma}} \cdot \underline{n}) \cdot \underline{n} = \underline{\underline{\sigma}} : (\underline{n} \otimes \underline{n}), \tag{1.14}$$

$$\underline{\sigma}_t = \underline{\underline{\sigma}} \cdot \underline{n} - \sigma_n \underline{n}. \tag{1.15}$$

Then, using the gap function, the intuitive contact conditions can be summarized in a local and computationally usable form:

- **Non-penetration:**
$$g \geq 0. \tag{1.16}$$

- **No adhesion** (or unilateral constraint); only compressive normal stress is admissible:
$$\sigma_n \leq 0. \tag{1.17}$$

- **Complementarity condition.** Contact pressure and gap cannot be simultaneously non-zero:
$$g\,\sigma_n = 0. \tag{1.18}$$

- **No shear transfer (frictionless contact)**. The tangential component of the traction vector vanishes (this condition is automatically verified):
$$\underline{\sigma}_t = \underline{\mathbf{0}}. \tag{1.19}$$

This set of conditions is called Hertz-Signorini-Moreau conditions[2] In optimization theory, the same complementarity structure is referred as Karush-Kuhn-Tucker[3] or KKT conditions.

$$\boxed{g \geq 0, \qquad \sigma_n \leq 0, \qquad g\,\sigma_n = 0.} \tag{1.20}$$

These conditions are graphically illustrated in Figure 1.5.

Alternatively, one can use contact pressure $p = -\sigma_n$ instead of negative normal contact traction, thus leading to

$$g \geq 0, \qquad p \geq 0, \qquad pg = 0. \tag{1.21}$$

The complementarity condition can be sometimes written $g \perp p$.

[2] **Heinrich Rudolf Hertz** (1857–1894) first formulated and solved the frictionless contact problem between elastic ellipsoidal bodies. **Antonio Signorini** (1888–1963) provided a general and rigorous mathematical formulation of contact constraints. **Jean Jacques Moreau** (1923–2014) reformulated contact as a non-smooth optimization problem and introduced pseudo-potentials in contact mechanics.

[3] **William Karush** (1917–1997) and **Harold William Kuhn** (1925-2014) are American mathematicians, and **Albert William Tucker** (1905–1995) is a Canadian mathematician.

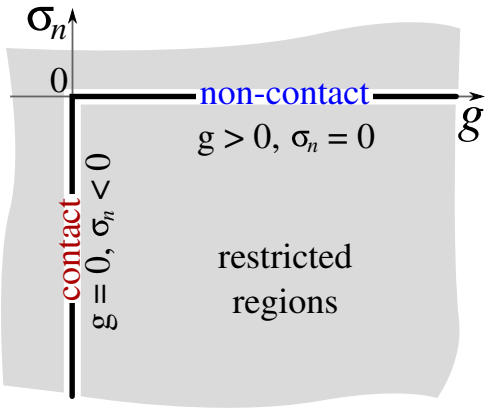

Figure 1.5: Normal (frictionless) contact conditions: non-penetration, compressive normal stress only, and complementarity between gap and contact pressure.

1.3 The Contact Problem

Preliminary formulation of the contact problem. The question that we start to address here is how to integrate contact constraints into the boundary value problem of two deformable bodies that may come into contact (see Figure 1.1). In general case, the contact constraints cannot be integrated as Dirichlet or Neumann boundary conditions, because the contact pressure and even the contact zone are not known in advance. Here, we give a preliminary formulation for the contact problem.

Contact problem formulation: Find a contact pressure[4] $p(\underline{\boldsymbol{x}}) \geq 0$ such that when applied on the (a priori unknown) contact surfaces $\Gamma_c^1 \subset \partial\Omega_1$ and $\Gamma_c^2 \subset \partial\Omega_2$, produces a deformed configuration which verifies Hertz-Signorini-Moreau conditions at all surface points $\partial\Omega_1, \partial\Omega_2$:

$$g \geq 0, \qquad p \geq 0, \qquad pg = 0 \qquad \forall \underline{\boldsymbol{x}} \in \partial\Omega_1, \partial\Omega_2 \tag{1.22}$$

Unknown contact zone. A fundamental difficulty is that the contact regions Γ_c^1 and Γ_c^2 are not known in advance. They themselves are unknowns of the problem.

Related direct problem. Starting from the problem of finding a relevant contact pressure verifying contact constraints, we can formulate another problem, which would be very relevant for further development.

Direct problem: *Given p on $\Gamma_c \subset \partial\Omega$, determine the corresponding displacement field $\underline{\boldsymbol{u}}$ in associated Ω.*

If the displacement field were known, one could compute the induced stress and therefore the contact pressure. The essence of contact mechanics lies in solving these two aspects simultaneously is such a way that they verify contact constraints.

This problem would be to complex to be solved analytically for arbitrary solid and arbitrary load. But it can be solved under some strong assumptions: (i) the solid can be locally approximated by a half-plane in 2D or a half-space in 3D; (ii) the problem remains linearly elastic so the superposition principle can be used. Under these assumptions, to address the formulated problem, we simply need to construct a so-called fundamental solution for a concentrated force on the surface and then by integrating it we can find the solution of the direct problem.

Let us first derive the fundamental solution for a plane problem, known as *Flamant solution* and sometime referred as *Kelvin solution*.

[4] We need to remember that at every surface point the pressure is applied along the normal $\underline{\boldsymbol{n}}$; since we are formulating the contact in small deformations and assuming that the deformed configuration and the reference one coincide, the normals from the reference configuration could be used, it leads however to some seeming ambiguity, because we do want to verify that the deformed solids do not penetrate which requires to truly distinguish the reference and the current configurations. This ambiguity can be fully resolved only if the contact is formulated with respect to the deformed normal, which makes the problem even more non-linear. Therefore, here for the sake of simplicity we stay with the classical definition and define the normals in the reference configuration.

1.4 Fundamental solution in 2D: Flamant solution

1.4.1 Problem statement

In Fig. 1.6 an elastic half-plane, Young's modulus E and Poisson's ratio ν, is shown. On its surface, a semi-circular groove of radius r is loaded by a distributed pressure $p(\theta) = p_0 \cos(\theta)$.

Problem: Find an induced stress state, deformation state and displacement field. Obtain asymptotic results for $r \to 0$ assuming that the resulting vertical force remains fixed.

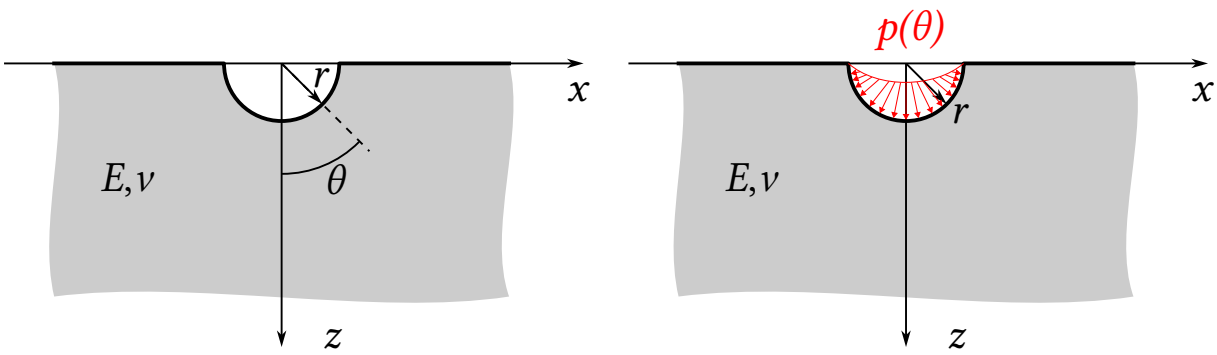

Figure 1.6: Elastic half-plane with a semi-circular groove on its surface subject to a distributed pressure $p(\theta)$

1.4.2 Stress tensor distribution

The stress state is given by the following tensor in polar coordinates

$$\underline{\underline{\sigma}} = -\frac{\alpha \cos(\theta)}{r}\left(\underline{e}_r \otimes \underline{e}_r + \nu \underline{e}_z \otimes \underline{e}_z\right), \tag{1.23}$$

where $\alpha = r_0 p_0$. Note, that we assumed a *plane-strain* formulation which makes more sense than a plane-stress one. The reason is that the latter makes sense for thin structure, but since in contact problem we have compressive loads, thin structures easily buckle, therefore, classically, the Flamant problem in contact is solved for the plane-strain formulation.

The integral of the stress vector over the circular hole gives:

$$-\int_{-\pi/2}^{\pi/2} \underline{\underline{\sigma}} \cdot \underline{e}_r r_0 d\theta = \frac{\alpha\pi}{2}\underline{e}_y = F\underline{e}_y, \tag{1.24}$$

then

$$\alpha = \frac{2F}{\pi}, \tag{1.25}$$

where F is the linear density of applied normal force.

1.4.3 Strain tensor distribution

The strain tensor is given by

$$\underline{\underline{\varepsilon}} = -\frac{\alpha \cos(\theta)}{rE}\left[(1-\nu^2)\underline{e}_r \otimes \underline{e}_r - \nu(1+\nu)\underline{e}_\theta \otimes \underline{e}_\theta\right] \tag{1.26}$$

1.4.4 Displacement field

The radial displacement can be found by integrating $\varepsilon_{rr} = \partial u_r/\partial r$:

$$u_r = -\frac{\alpha\cos(\theta)(1-\nu^2)}{E}\log(r) + f(\theta), \tag{1.27}$$

where $f(\theta)$ is an uknown function. The second displacement component u_θ can be found through the expression of $\varepsilon_{\theta\theta} = \frac{1}{r}(\partial u_\theta/\partial\theta + u_r)$, which after integration takes the form:

$$u_\theta = -\frac{\alpha\sin(\theta)\nu(1+\nu)}{E} + \frac{\alpha\sin(\theta)(1-\nu^2)}{E}\log(r) - \int f(\theta)d\theta + g(r), \tag{1.28}$$

where $g(r)$ is another unknown function. So, we have two unknown functions and will need at least two equations to identify them. The both can be obtained from the fact that $\varepsilon_{r\theta} = 0$, in polar coordinates it has a form:

$$\varepsilon_{r\theta} = \frac{1}{2}\left[\frac{1}{r}\left(\frac{\partial u_r}{\partial\theta} - u_\theta\right) + \frac{\partial u_\theta}{\partial r}\right] = 0, \tag{1.29}$$

or equvalently for non-zero r

$$\frac{\partial u_r}{\partial\theta} - u_\theta + r\frac{\partial u_\theta}{\partial r} = 0. \tag{1.30}$$

We substitute (1.27) and (1.28) in it and obtain:

$$\frac{\partial f(\theta)}{\partial\theta} + \frac{\alpha\sin(\theta)\nu(1+\nu)}{E} + \int f(\theta)d\theta - g(r) - \frac{\alpha\sin(\theta)(1-\nu^2)}{E} + r\frac{\partial g(r)}{\partial r} = 0. \tag{1.31}$$

After grouping terms that depend solely on r and on θ we obtain the following equality:

$$\frac{\partial f(\theta)}{\partial\theta} + \int f(\theta)d\theta - \frac{\alpha\sin(\theta)(1+\nu)(1-2\nu)}{E} = g(r) - r\frac{\partial g(r)}{\partial r}. \tag{1.32}$$

Thanks to this separation of variables, both the left and the right hand sides should be equal to the same constant C, and we obtain two equations needed to find $f(\theta)$ and $g(r)$:

$$\begin{cases} \dfrac{\partial f(\theta)}{\partial\theta} + \displaystyle\int f(\theta)d\theta - \frac{\alpha\sin(\theta)(1+\nu)(1-2\nu)}{E} = C \\ g(r) - r\dfrac{\partial g(r)}{\partial r} = C \end{cases} \tag{1.33}$$

We take the derivative of the first and obtain:

$$\frac{\partial^2 f(\theta)}{\partial\theta^2} + f(\theta) = \frac{\alpha\cos(\theta)(1+\nu)(1-2\nu)}{E}. \tag{1.34}$$

The solution of the homogeneous (for zero right hand part) linear second-order differential equation is given by:

$$f_0(\theta) = A\cos(\theta) + B\sin(\theta), \tag{1.35}$$

the particular solution we can seek in the form:

$$f_*(\theta) = h(\theta)\sin(\theta), \tag{1.36}$$

which after its substitution in (1.34) gives:

$$\frac{\partial^2 h}{\partial\theta^2}\sin(\theta) + 2\frac{\partial h}{\partial\theta}\cos(\theta) = \frac{\alpha\cos(\theta)(1+\nu)(1-2\nu)}{E}, \tag{1.37}$$

therefore

$$\frac{\partial^2 h}{\partial\theta^2} = 0 \quad \text{and} \quad 2\frac{\partial h}{\partial\theta} = \frac{\alpha(1+\nu)(1-2\nu)}{E}, \tag{1.38}$$

since we have already $B\sin(\theta)$ in our solution of the homogeneous equation f_0, we keep only the linear term of function $h(\theta) = \alpha(1+\nu)(1-2\nu)\theta/(2E)$:

$$f_*(\theta) = \frac{\alpha(1+\nu)(1-2\nu)}{2E}\theta\sin(\theta). \tag{1.39}$$

The full solution for $f(\theta)$ is then given by:

$$\boxed{f(\theta) = A\cos(\theta) + B\sin(\theta) + \frac{\alpha(1+\nu)(1-2\nu)}{2E}\theta\sin(\theta)}. \tag{1.40}$$

For the function $g(r)$, from Eq. (1.33) it immediately follows that

$$g(r) = Er + C. \tag{1.41}$$

Finally, the displacements are given by:

$$u_r = -\frac{\alpha\cos(\theta)(1-\nu^2)}{E}\log(r) + \underbrace{A\cos(\theta) + B\sin(\theta)}_{\text{Rigid body displacement}} + \frac{\alpha(1+\nu)(1-2\nu)}{2E}\theta\sin(\theta) \tag{1.42}$$

$$\begin{aligned} u_\theta = &-\frac{\alpha\sin(\theta)\nu(1+\nu)}{E} + \frac{\alpha\sin(\theta)(1-\nu^2)}{E}\log(r) \underbrace{-A\sin(\theta) + B\cos(\theta)}_{\text{Rigid body displacement}} - \frac{\alpha(1+\nu)(1-2\nu)}{2E}\sin(\theta) + \\ &+ \frac{\alpha(1+\nu)(1-2\nu)}{2E}\theta\cos(\theta) + \underbrace{Er}_{\text{Rigid body rotation}} + C \end{aligned} \tag{1.43}$$

If we remove rigid body motion, we obtain the following displacements on the surface:

$$\boxed{u_x = -\frac{F(1+\nu)(1-2\nu)}{2E}\text{sign}(x)} \tag{1.44}$$

$$\boxed{u_y = \frac{2F(1-\nu^2)}{\pi E}\log(|x|) + C} \tag{1.45}$$

Note that $u_x = u_r\underline{\boldsymbol{e}}_r \cdot \underline{\boldsymbol{e}}_x$ for $\theta = \pm\pi/2$, and $u_y = u_\theta\underline{\boldsymbol{e}}_\theta \cdot \underline{\boldsymbol{e}}_y$ for $\theta = \pm\pi/2$. We also used the expression for α from Eq. (1.25).

By analogy, similar results could be obtained for the tangential force if instead of applying pressure in form $p = p_0\cos(\theta)$, the pressure $p = p_0\sin(\theta)$ is used.

1.4.5 Concentrated Forces on a Half-Plane (Flamant Solution): summary

Normal concentrated force. We recall that we are in plane strain conditions and the elastic half-plane is loaded by a compressive concentrated normal force N (Figure 1.7, left). The stress field in polar coordinates (r, θ) reads

$$\sigma_r = -\frac{2N}{\pi}\frac{\cos\theta}{r}. \tag{1.46}$$

In Cartesian coordinates, the in-plane stresses are

$$\boxed{\sigma_x = -\frac{2N}{\pi}\frac{x^2y}{(x^2+y^2)^2}, \qquad \sigma_y = -\frac{2N}{\pi}\frac{y^3}{(x^2+y^2)^2}, \qquad \sigma_{xy} = -\frac{2N}{\pi}\frac{xy^2}{(x^2+y^2)^2}.} \tag{1.47}$$

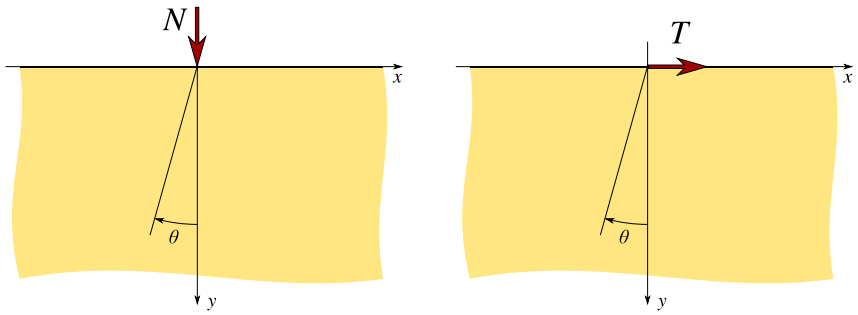

Figure 1.7: Normal and tangential concentrated forces applied to an elastic half-space (Flamant problem).

and $\sigma_z = \nu(\sigma_x + \sigma_y)$. If the normal force is applied at $x = s$, we get

$$\boxed{\sigma_x(x,y) = -\frac{2N}{\pi}\frac{(x-s)^2 y}{((x-s)^2+y^2)^2}, \qquad \sigma_y(x,y) = -\frac{2N}{\pi}\frac{y^3}{((x-s)^2+y^2)^2}, \qquad \sigma_{xy}(x,y) = -\frac{2N}{\pi}\frac{(x-s)y^2}{((x-s)^2+y^2)^2}.} \tag{1.48}$$

This form will be helpful for further development.

The displacement field in polar coordinates is

$$u_r = \frac{1+\nu}{\pi E} N\cos\theta\,[2(1-\nu)\ln r - (1-2\nu)\theta\tan\theta] + C\cos\theta, \tag{1.49}$$

$$u_\theta = \frac{1+\nu}{\pi E} N\sin\theta\,[2(1-\nu)\ln r - 2\nu + (1-2\nu)(1-2\theta\,\mathrm{ctan}\theta)] - C\sin\theta, \tag{1.50}$$

where E is Young's modulus, ν Poisson's ratio, and C is an integration constant related to rigid-body motion which can be omitted.

On the free surface ($y = 0$) which corresponds to $\theta = \pm\pi/2$, the displacements simplify to

$$\boxed{u_x = -\frac{N(1+\nu)(1-2\nu)}{2E}\,\mathrm{sign}(x), \qquad u_y = \frac{2N(1-\nu^2)}{\pi E}\log|x|} \tag{1.51}$$

If the normal force is applied at $x = s$, we get

$$\boxed{u_x(x) = -\frac{N(1+\nu)(1-2\nu)}{2E}\,\mathrm{sign}(x-s), \qquad u_y(x) = \frac{2N(1-\nu^2)}{\pi E}\log|x-s|} \tag{1.52}$$

Tangential concentrated force. If a horizontal (tangential) force T is applied at the origin (Figure 1.7, right), the stress field becomes

$$\sigma_r = \frac{2T}{\pi}\frac{\sin\theta}{r}, \tag{1.53}$$

and in Cartesian coordinates

$$\boxed{\sigma_x = -\frac{2T}{\pi}\frac{x^3}{(x^2+y^2)^2}, \qquad \sigma_y = -\frac{2T}{\pi}\frac{xy^2}{(x^2+y^2)^2}, \qquad \sigma_{xy} = -\frac{2T}{\pi}\frac{x^2 y}{(x^2+y^2)^2}.} \tag{1.54}$$

If the tangential load is applied at $x = s$, we get the following form

$$\boxed{\sigma_x(x,y) = -\frac{2T}{\pi}\frac{(x-s)^3}{((x-s)^2+y^2)^2}, \qquad \sigma_y(x,y) = -\frac{2T}{\pi}\frac{(x-s)y^2}{((x-s)^2+y^2)^2}, \qquad \sigma_{xy}(x,y) = -\frac{2T}{\pi}\frac{(x-s)^2 y}{((x-s)^2+y^2)^2}.} \tag{1.55}$$

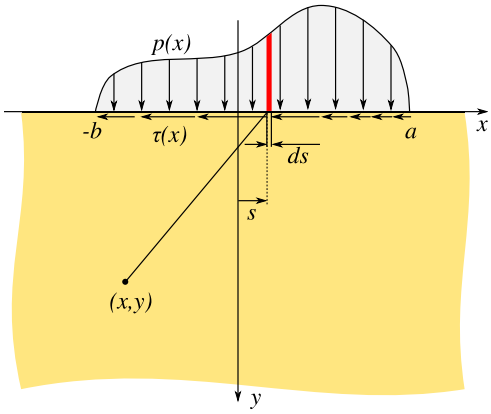

Figure 1.8: Distributed normal and tangential tractions applied on the surface of an elastic half-plane.

The displacement field in polar coordinates reads

$$u_r = -\frac{1+\nu}{\pi E} T \sin\theta \left[2(1-\nu)\ln r - (1-2\nu)\theta \operatorname{ctan}\theta\right] - C\sin\theta, \tag{1.56}$$

$$u_\theta = \frac{1+\nu}{\pi E} T \cos\theta \left[2(1-\nu)\ln r - 2\nu + (1-2\nu)(1+2\theta\tan\theta)\right] + C\cos\theta. \tag{1.57}$$

On the free surface ($y = 0$), for the tangent force applied at $x = 0$, the displacements take the form

$$\boxed{u_x = -\frac{2T(1-\nu^2)}{\pi E}\log|x| + C, \qquad u_y = \frac{T(1+\nu)(1-2\nu)}{2E}\operatorname{sign}(x).} \tag{1.58}$$

In case of the tangent force applied at $x = s$, we obtain the following form

$$\boxed{u_x(x) = -\frac{2T(1-\nu^2)}{\pi E}\log|x-s| + C, \qquad u_y(x) = \frac{T(1+\nu)(1-2\nu)}{2E}\operatorname{sign}(x-s).} \tag{1.59}$$

1.5 Distributed Surface Loads

From concentrated to distributed loads Using the superposition principle, the solution for a concentrated force can be extended to a distributed surface traction. Let $p(x)$ denote a normal pressure distribution and $\tau(x)$ a tangential traction distribution applied on the surface $y = 0$ over the interval $[-b, a]$ (see Figure 1.8).

By stating that infinitesimal force contributions for the normal and the tangetial forces read

$$dN(x) = p(x)\,dx, \qquad dT(x) = \tau(x)\,dx, \tag{1.60}$$

we will use equations derived for the concentrated normal and tangential forces. So, the total stress and displacement fields are obtained by integrating the Flamant fundamental solutions.

1.5.1 Stress field

The in-plane stresses are given by the following integrals

$$\sigma_x(x,y) = -\frac{2y}{\pi}\int_{-b}^{a} \frac{p(s)(x-s)^2}{\left((x-s)^2+y^2\right)^2}\,ds - \frac{2}{\pi}\int_{-b}^{a} \frac{\tau(s)(x-s)^3}{\left((x-s)^2+y^2\right)^2}\,ds, \tag{1.61}$$

$$\sigma_y(x,y) = -\frac{2y^3}{\pi}\int_{-b}^{a} \frac{p(s)}{\left((x-s)^2+y^2\right)^2}\,ds - \frac{2y^2}{\pi}\int_{-b}^{a} \frac{\tau(s)(x-s)}{\left((x-s)^2+y^2\right)^2}\,ds, \tag{1.62}$$

$$\sigma_{xy}(x,y) = -\frac{2y^2}{\pi}\int_{-b}^{a}\frac{p(s)(x-s)}{\left((x-s)^2+y^2\right)^2}\,ds - \frac{2y}{\pi}\int_{-b}^{a}\frac{\tau(s)(x-s)^2}{\left((x-s)^2+y^2\right)^2}\,ds. \tag{1.63}$$

1.5.2 Surface displacements

On the surface $y = 0$, the tangential displacement u_x is

$$u_x(x,0) = -\text{sign}(x)\frac{(1-2\nu)(1+\nu)}{2E}\left[\int_{-b}^{x} p(s)\,ds - \int_{x}^{a} p(s)\,ds\right] - \frac{2(1-\nu^2)}{\pi E}\int_{-b}^{a}\tau(s)\ln|x-s|\,ds + C_1. \tag{1.64}$$

Differentiating along the surface eliminates the rigid-body constant and produces a simpler to manipulate equation:

$$\boxed{u_{x,x}(x,0) = -\text{sign}(x)\frac{(1-2\nu)(1+\nu)}{E}p(x) - \frac{2(1-\nu^2)}{\pi E}\int_{-b}^{a}\frac{\tau(s)}{x-s}\,ds.} \tag{1.65}$$

The normal displacement, is given by the following equation:

$$u_y(x,0) = \text{sign}(x)\frac{(1-2\nu)(1+\nu)}{2E}\left[\int_{-b}^{x}\tau(s)\,ds - \int_{x}^{a}\tau(s)\,ds\right] - \frac{2(1-\nu^2)}{\pi E}\int_{-b}^{a}p(s)\ln|x-s|\,ds + C_2. \tag{1.66}$$

Again, differentiating by the coordinate x gives a simpler form:

$$\boxed{u_{y,x}(x,0) = \text{sign}(x)\frac{(1-2\nu)(1+\nu)}{E}\tau(x) - \frac{2(1-\nu^2)}{\pi E}\int_{-b}^{a}\frac{p(s)}{x-s}\,ds.} \tag{1.67}$$

All these equations are very helpful for all two-dimensional problems with free surface. And we will use them in our practical work **??**.

1.5.3 Inverse Problem

From surface kinematics to tractions From the previous expressions for the surface derivatives $u_{x,x}(x,0)$ and $u_{y,x}(x,0)$, we can eliminate the displacement terms and express the singular integrals directly in terms of tractions.

After rearrangement, we obtain the coupled relations

$$\text{p.v.}\int_{-b}^{a}\frac{\tau(s)}{x-s}\,ds = -\frac{\pi(1-2\nu)}{2(1-\nu)}\,p(x) - \frac{\pi E}{2(1-\nu^2)}\,u_{x,x}(x,0), \tag{1.68}$$

$$\text{p.v.}\int_{-b}^{a}\frac{p(s)}{x-s}\,ds = \frac{\pi(1-2\nu)}{2(1-\nu)}\,\tau(x) - \frac{\pi E}{2(1-\nu^2)}\,u_{y,x}(x,0). \tag{1.69}$$

Note that p.v. in the integral denotes the *Cauchy principal value*. The principal value of a singular integral with the integrand diverging at $x = x^*$ is given by

$$F = \text{p.v.}\int_{-b}^{a} f(s)ds = \lim_{\varepsilon\to 0}\left[\int_{-b}^{x^*-\varepsilon} f(s)ds + \int_{x^*+\varepsilon}^{a} f(s)ds\right]$$

Reduction to a singular integral equation If, on the contact interface, we prescribe the right-hand side, i.e. either

$$(p,\ u_{x,x}) \qquad \text{or} \qquad (\tau,\ u_{y,x}),$$

then the problem reduces to a single singular integral equation of Cauchy type (of the first kind):

$$\text{p.v.} \int_{-b}^{a} \frac{\mathcal{F}(s)}{x-s}\, ds = \mathcal{U}(x), \tag{1.70}$$

where under the integral we have the unknown function $\mathcal{F}$ which can be interpreted as $\tau(s)$ if we prescribed $\mathcal{U}$ through $(p,\ u_{x,x})$, or $\mathcal{F} = p(s)$ if we prescribed $\mathcal{U}$ through $(\tau,\ u_{y,x})$. In Equation (1.70) the right hand side $\mathcal{U}$ can be seen as the finite ilbert transform of $\mathcal{F}$, so to find $\mathcal{F}$ from $\mathcal{U}$ we need to apply inverse Hilbert transform.

General solution for a symmetric interval In the particular case $a = b$, i.e. over the symmetric interval $[-a, a]$, the general solution reads

$$\mathcal{F}(x) = \frac{1}{\pi^2\sqrt{a^2-x^2}}\text{p.v.}\int_{-a}^{a} \frac{\sqrt{a^2-s^2}\,\mathcal{U}(s)}{x-s}\, ds + \frac{C}{\pi\sqrt{a^2-x^2}}, \text{ with } C = \int_{-a}^{a} \mathcal{F}(s)\, ds. \tag{1.71}$$

Thanks to this general solution of the inverse Hilbert transform we can already solve our first contact problems. In the insert below, we find the pressure field for three types of indenter: flat, wedge and parabolic.

🖍️ Examples. From indenter's shape to pressure.

In this insert, we demonstrate a solution for the inverse problem Equation (1.69) for three indenters: flat punch, wedge and parabolic indenter.

Flat Indenter Let us assume that we have a symmetric rigid flat indenter or half-width a which indents the surface with a force F. Let also assume that there are no tangential tractions $\tau(x) = 0$. Since the indenter is flat, then in the contact interface $u_{x,x} = 0$. So, we simply have $\mathcal{U} = 0$ and we search for the contact pressure $\mathcal{F} = p$. According to the solution Equation (1.71), we readily obtain the pressure in the contact interface under the rigid punch as

$$p_{\text{flat}}(x) = \frac{F}{\pi\sqrt{a^2-x^2}}. \tag{1.72}$$

Note that we used the fact that the constant C in Equation (1.71) is nothing but the integral of contact pressure $\mathcal{F} = p$ in the contact interface, i.e. the force density. The contact pressure of a flat indenter diverges at contact edges.

Wedge or Triangular Indenter For a triangular indenter given by equation $y = \tan(\alpha)|x|$, in absence of frictional forces, the right-hand side takes the form $\mathcal{U} = -\frac{\pi E}{2(1-\nu^2)}\tan(\alpha)\text{sign}(x)$. Then from Equation (1.71), the contact pressure is given by

$$p_{\text{tri}}(x) = \frac{-E\tan(\alpha)}{2\pi(1-\nu^2)\sqrt{a^2-x^2}}\text{p.v.}\int_{-a}^{a} \frac{\text{sign}(s)\,\sqrt{a^2-s^2}}{x-s}\, ds + \frac{F}{\pi\sqrt{a^2-x^2}}$$

where

$$F = \int_{-a}^{a} p(s)\, ds.$$

The integral can be evaluated

$$p_{\text{tri}}(x) = \frac{-E\tan(\alpha)}{2\pi(1-\nu^2)} \ln\left(\frac{a - \sqrt{a^2-x^2}}{a + \sqrt{a^2-x^2}}\right) + \frac{1}{\pi\sqrt{a^2-x^2}}\left(F - \frac{aE\tan(\alpha)}{(1-\nu^2)}\right)$$

To avoid spurious divergence at the edges of the contact zone $|x| = a$, the second term should vanish, i.e. the expression in brackets should vanish, resulting in the total force given by

$$F = \frac{aE\tan(\alpha)}{(1-\nu^2)}$$

and the pressure distribution is then given by

$$p_{\text{tri}}(x) = \frac{-E\tan(\alpha)}{2\pi(1-\nu^2)} \ln\left(\frac{a - \sqrt{a^2-x^2}}{a + \sqrt{a^2-x^2}}\right) \tag{1.73}$$

The contact pressure is singular at the center.

Parabolic Indenter For a parabolic indenter of curvature R given by equation $y = x^2/2R$ in absence of frictional forces, the right-hand side takes the form $\mathcal{U} = -\frac{\pi E}{2(1-\nu^2)} u_{x,x}(x,0) = -\frac{\pi E}{2(1-\nu^2)} x/R$. Then from Equation (1.71), the contact pressure is given by

$$p_{\text{parab}}(x) = \frac{-E}{2\pi(1-\nu^2)R\sqrt{a^2-x^2}} \int_{-a}^{a} \frac{s\sqrt{a^2-s^2}}{x-s}\, ds + \frac{F}{\pi\sqrt{a^2-x^2}}.$$

Evaluating the integral gives the following solution:

$$p_{\text{parab}}(x) = \frac{E}{2(1-\nu^2)R}\sqrt{a^2-x^2} + \frac{1}{\sqrt{a^2-x^2}}\left(\frac{F}{\pi} - \frac{a^2E}{4(1-\nu^2)R}\right).$$

From this form we can conclude, that the factor of the second term should vanish to avoid divergence of pressure at the boundary, i.e. the total force is given by

$$F = \frac{\pi a^2 E}{4(1-\nu^2)R}$$

and then the contact pressure in the interface is given by

$$p_{\text{parab}}(x) = \frac{Ea}{2(1-\nu^2)R}\sqrt{1-(x/a)^2}. \tag{1.74}$$

The obtained pressure is elliptic. This pressure is nothing but Hertzian contact solution in 2D; it will be presented in detail in **??**.
The three obtained solutions are plotted below, the pressure is normalized as $p' = 2ap/F$ and the coordinate is normalized as $x' = x/a$.

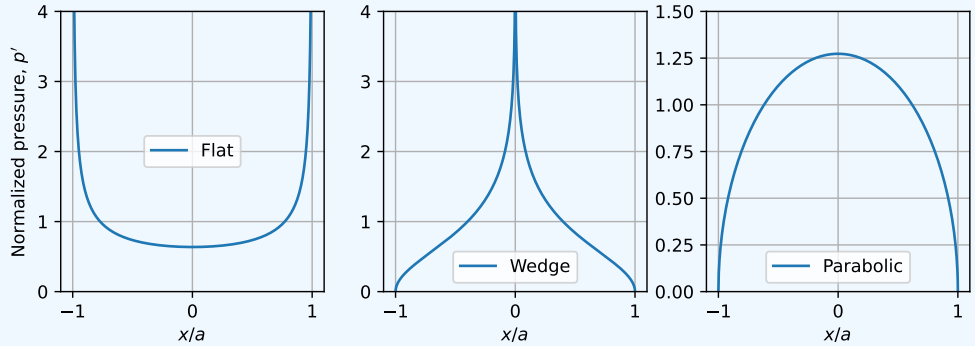

1.6 Three-Dimensional Half-Space Problem

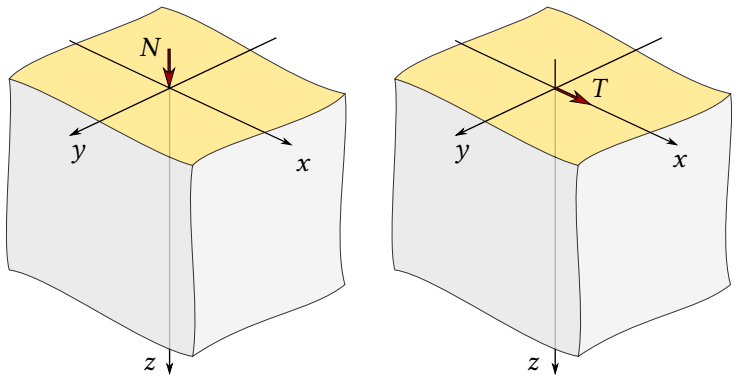

Figure 1.9: Boussinesq and Cerruti problems of concentrated forces on the half-space.

Analogy with Flamant's solution. The three-dimensional counterpart of Flamant's plane strain solution is the half-space subjected to a concentrated force applied at the surface, Figure 1.9. The fundamental solutions are due to Boussinesq (normal force) and Cerruti (tangential force). However, for the three-dimensional case the problem of undefined datum present in two-dimensional case disappears since the displacement decay at infinity.

We consider an isotropic elastic half-space occupying $z \geq 0$, characterized by shear modulus $G = E/(2(1+\nu))$ and Poisson's ratio ν.

Boussinesq solution The Boussinesq solution for a concentrated normal force F applied at $\{x', y'\}$ is given by the following expressions for the stresses at point $\{x, y, z\}$:

$$
\begin{aligned}
\rho &= \sqrt{(x-x')^2 + (y-y')^2 + z^2} \\
r &= \sqrt{(x-x')^2 + (y-y')^2} \\
\sigma_x^B &= \frac{N}{2\pi}\left(\frac{1-2\nu}{r^2}\left(\frac{1-z/\rho}{r^2}\left((x-x')^2 - (y-y')^2\right) + \frac{z(y-y')^2}{\rho^3}\right) - \frac{3z(x-x')^2}{\rho^5}\right) \\
\sigma_y^B &= \frac{N}{2\pi}\left(\frac{1-2\nu}{r^2}\left(\frac{1-z/\rho}{r^2}\left((y-y')^2 - (x-x')^2\right) + \frac{z(x-x')^2}{\rho^3}\right) - \frac{3z(y-y')^2}{\rho^5}\right) \\
\sigma_z^B &= -3\frac{N}{2\pi}\frac{z^3}{\rho^5} \\
\sigma_{xy}^B &= \frac{N}{2\pi}(x-x')(y-y')\left(\frac{1-2\nu}{r^2}\left(\frac{1-z/\rho}{r^2} - \frac{z}{\rho^3}\right) - \frac{3z}{\rho^5}\right) \\
\sigma_{xz}^B &= -3\frac{N}{2\pi}\frac{z^2(x-x')}{\rho^5} \\
\sigma_{yz}^B &= -3\frac{N}{2\pi}\frac{z^2(y-y')}{\rho^5}.
\end{aligned}
$$

Associated displacements on the surface of the half-space at $\{x, y\}$ are given by:

$$u_x^B = \frac{N(1-2\nu)}{4\pi G}\frac{x-x'}{r^2}$$
$$u_y^B = \frac{N(1-2\nu)}{4\pi G}\frac{y-y'}{r^2}$$
$$u_z^B = \frac{N(1-\nu)}{2\pi G}\frac{1}{r} = \frac{F(1-\nu^2)}{\pi E r},$$

note that the vertical displacement is of positive sign since the axis OZ is oriented downwards in the half-space.

Full displacement field. In the half-space ($z > 0$), the displacement components are

$$u_x = \frac{N}{4\pi G}\left(\frac{xz}{r^3} - (1-2\nu)\frac{x}{r(r+z)}\right), \tag{1.75}$$

$$u_y = \frac{N}{4\pi G}\left(\frac{yz}{r^3} - (1-2\nu)\frac{y}{r(r+z)}\right), \tag{1.76}$$

$$u_z = \frac{N}{4\pi G}\left(\frac{z^2}{r^3} + \frac{2(1-\nu)}{r}\right). \tag{1.77}$$

These expressions clearly exhibit the r^{-1} singular behavior near the load point.

Generalized representation These expressions could be reformulated as follows:

$$\boxed{\sigma_{ij}^B(x, y, z) = NS_{ij}^B(x-x', y-y', z, \nu)}$$

$$\boxed{u_i^B(x, y) = ND_i^B(x-x', y-y', G, \nu)}$$

where $S_{ij}^B(\Delta x, \Delta y, z, \nu)$ and $D_i^B(\Delta x, \Delta y, G, \nu)$ are the Boussinesq kernels for stresses and displacements, respectively. Note that even though we included the Poisson ratio ν in the expressions for the Boussinesq kernels, $\sigma_z, \sigma_{xz}, \sigma_{yz}$ components are independent of ν.

1.6.1 Cerruti solution

The Cerruti solution for a concentrated tangential force T_x applied at $\{x', y'\}$ is given by the following expressions for the stresses at point $\{x, y, z\}$:

$$\begin{aligned}
\sigma_x^C &= \frac{T_x}{2\pi}\left(-\frac{3(x-x')^3}{\rho^5}+\right.\\
&\quad \left.+\,(1-2\nu)\left(\frac{x-x'}{\rho^3}-\frac{3(x-x')}{\rho(\rho+z)^2}+\frac{(x-x')^3}{\rho^3(\rho+z)^2}+\frac{2(x-x')^3}{\rho^2(\rho+z)^3}\right)\right)\\
\sigma_y^C &= \frac{T_x}{2\pi}\left(-\frac{3(x-x')(y-y')^2}{\rho^5}+\right.\\
&\quad \left.+\,(1-2\nu)\left(\frac{x-x'}{\rho^3}-\frac{x-x'}{\rho(\rho+z)^2}+\frac{(x-x')(y-y')^2}{\rho^3(\rho+z)^2}+\frac{2(x-x')(y-y')^2}{\rho^2(\rho+z)^3}\right)\right)\\
\sigma_z^C &= -\frac{3T_x}{2\pi}\frac{(x-x')z^2}{\rho^5}\\
\sigma_{xy}^C &= \frac{T_x}{2\pi}\left(-\frac{3(x-x')^2(y-y')}{\rho^5}+\right.\\
&\quad \left.+\,(1-2\nu)\left(-\frac{(y-y')}{\rho(\rho+z)^2}+\frac{(x-x')^2(y-y')}{\rho^3(\rho+z)^2}+\frac{2(x-x')^2(y-y')}{\rho^2(\rho+z)^3}\right)\right)\\
\sigma_{xz}^C &= -\frac{3T_x}{2\pi}\frac{(x-x')(y-y')z}{\rho^5}\\
\sigma_{yz}^C &= -\frac{3T_x}{2\pi}\frac{(x-x')^2z}{\rho^5}
\end{aligned}$$

Associated displacements on the surface of the half-space at $\{x, y\}$ are given by:

$$\begin{aligned}
u_x^C &= \frac{T_x}{4\pi G}\left(\frac{1}{r}-\frac{(x-x')^2}{r^3}+(1-2\nu)\left(\frac{1}{r}-\frac{(x-x')^2}{r^3}\right)\right)\\
u_y^C &= -\frac{T_x}{4\pi G}\cdot\frac{(x-x')(y-y')2\nu}{r^3}\\
u_z^C &= \frac{T_x}{4\pi G}\cdot\frac{(1-2\nu)(x-x')}{r^2}.
\end{aligned}$$

Generalized representation By analogy with the Boussinesq solution, these expressions could be reformulated as follows:

$$\boxed{\sigma_{ij}^C(x,y,z) = T_x S_{ij}^C(x-x', y-y', z, \nu)}$$

$$\boxed{u_i^C(x,y) = T_x D_i^C(x-x', y-y', G, \nu)}$$

where $S_{ij}^C(\Delta x, \Delta y, z, \nu)$ and $D_i^C(\Delta x, \Delta y, G, \nu)$ are the Cerruti kernels for stresses and displacements, respectively. Note that even though we included the Poisson ratio ν in the expressions for the Boussinesq kernels, $\sigma_z, \sigma_{xz}, \sigma_{yz}$ components are independent of ν.

1.6.2 Integration of Boussinesq and Cerruti solutions

Consider a pressure distribution $p(x, y)$ and tangential OX tractions $\underline{q}(x, y) = q(x, y)\underline{e}_x$ applied on region Ω of the surface of the half-space. Assuming linear elasticity, we can superpose the Boussinesq and Cerruti solutions to obtain the following expressions for the stresses at point $\{x, y, z\}$:

$$\sigma_{ij}(x,y,z) = \int_\Omega \Big(S_{ij}^B(x-x', y-y', z, \nu)p(x', y') + S_{ij}^C(x-x', y-y', z, \nu)q(x', y')\Big)\,dx'dy'. \tag{1.78}$$

For the displacements on the surface, the integrals are the following:

$$u_i(x,y) = \int_\Omega \left(D_i^B(x-x', y-y', G, \nu) p(x', y') + D_i^C(x-x', y-y', G, \nu) q(x', y') \right) dx' dy'. \tag{1.79}$$

1.6.3 Axisymmetric pressure distribution.

In many practical applications presenting axial symmetry, it is helpful to have a simplified convolution (Johnson 1987, Eq. (3.96a)). Consider a problem where the pressure is axisymmetric $p = p(r)$, then the resulting vertical displacement is given by

$$u_z(r) = \frac{4(1-\nu^2)}{\pi E} \int_0^\infty \frac{\rho}{\rho + r} p(\rho)\, K(k(r,\rho))\, d\rho \tag{1.80}$$

where r and ρ are the radial coordinates and the modulus k of the complete elliptic integral of the first kind $K(k)$ is given by:

$$k(r,\rho) = \frac{4\rho r}{(r+\rho)^2}, \quad K(k) = \int_0^{\pi/2} [1 - k \sin^2(t)]^{-1/2}\, dt. \tag{1.81}$$

1.7 Classification of Contact

Types of contact Contact problems differ by geometry, by whether the contact zone is known in advance, and by the presence of friction or adhesion. Typical geometrical configurations are illustrated in Figure 1.11 and include three main cases. First, a *conformal contact* - the contact geometry is predefined, it could be a cube on a flat, or a sphere in a spherical cavity of the same size. For this contact, the contact area is known and it seriously simplifies the problem. This type of contact may also occur when the initial geometry is non-conformal but the load is so large that the interface closes and full contact is achieved; this situation is however different since before reaching the conformal configuration the non-linear case should be treated. The second type, is a *line contact* - the situation where the first touch happens along a line, for example, a cylinder contacting a plane along its axis; all contact problems in 2D are line contacts. The third type, is the *point contact*, the situation when the first touch happens at a single point and the contact area spreads out under increasing load.

Another distinction between contact types resides in the interface behavior, the mechanical character of contact. The contact can be approximated to be *frictionless* (no tangential tractions transmitted in the interface) and *unilateral* (equiv. non-adhesive). This is relatively simple situation because the problem is conservative; it can typically be formulated as an energy minimization problem with Hertz-Signorini-Moreau constraints. The contact can be *adhesive* and experience tensile stresses in the contact interface; this behaviour can governed by different models which will be studied in **??**. Finally, the contact can be *frictional*, meaning that it has some tangential forces opposing the motion that appear in the interface. Both adhesive and frictional problems are not conservative, i.e. their solution depends on the history of loading. It means that the path-dependent history for all points must be tracked from first touch to the current state.

1.8 Analogy with Boundary Conditions

The contact problem is in general complex and non-linear. However, there are situations in which the true contact problem can be replaced by a simpler one by using either classical or more tricky boundary conditions. This analogy is illustrated in Figure 1.11 and Figure 1.12.

Flat geometry Consider the compression of a cylinder between two rigid plates (see Figure 1.11). Different contact idealizations correspond to different boundary conditions:

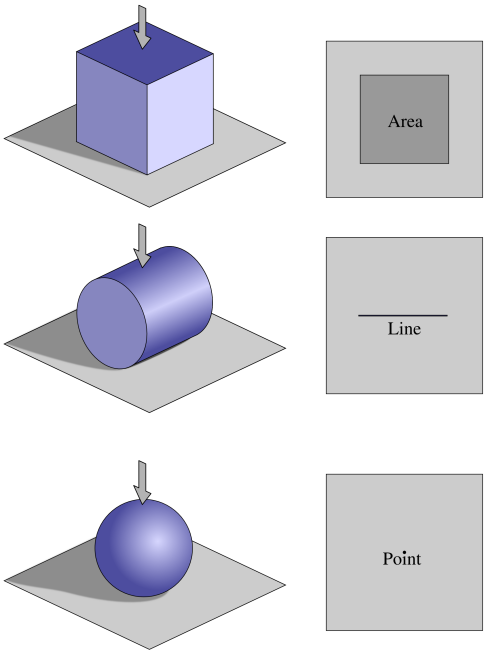

Figure 1.10: From top to the bottom: examples of conformal contact, line contact and point contact configurations.

- **Frictionless contact:** the normal displacement is prescribed,

$$u_z(\text{bottom}) = 0, \quad u_z(\text{top}) = -u_0, \tag{1.82}$$

  while tangential tractions vanish.

- **Full stick (perfect adhesion):** the full displacement vector is prescribed,

$$\underline{\boldsymbol{u}}(\text{bottom}) = 0, \quad \underline{\boldsymbol{u}}(\text{top}) = -u_0 \underline{\boldsymbol{e}}_z, \tag{1.83}$$

  i.e. both normal and tangential motion are constrained.

In the same manner, we can model the effect of a rigid flat indenter whatever its in-plane section is (see Figure 1.11). We simply need to impose the vertical displacement on the deformable surface over the region repeting the flat indenter shape $\mathcal{I}$:

$$u_z(\mathcal{I}) = -u_0. \tag{1.84}$$

Curved geometry For cylindrical or spherical surfaces in case of conformal contact, it is natural to express the constraint in polar or spherical coordinates, respectively. For example, for a deformable cylinder embedded in a force fit into a cylindrical hole and fully closing contact gap, it makes sense to impose the compatibility condition $u_r^1(\theta) - u_r^2(\theta) = 0$ between cylinders 1 and 2; these conditions replace the general contact constraints.

If under sufficiently high pressure, we have *complete* frictionless contact between a deformable solid and a rigid profile (Figure 1.12) given by equation

$$y = f(x) \tag{1.85}$$

the kinematic condition to be imposed in the contact interface reads

$$(\underline{\boldsymbol{X}} + \underline{\boldsymbol{u}}) \cdot \underline{\boldsymbol{e}}_y = f\Big((\underline{\boldsymbol{X}} + \underline{\boldsymbol{u}}) \cdot \underline{\boldsymbol{e}}_x\Big) \quad \Leftrightarrow \quad u_y = f(X + u_x) - Y. \tag{1.86}$$

Thus, contact can be viewed as a nonlinear geometric constraint on the current configuration, which can be linearized around the current configuration $u_x = u_x^0 + \Delta u_x$ and $u_y = u_y^0 + \Delta u_y$ resulting in

$$\Delta u_y = \left.\frac{\partial f}{\partial x}\right|_{x=X+u_x^0} \Delta u_X. \tag{1.87}$$

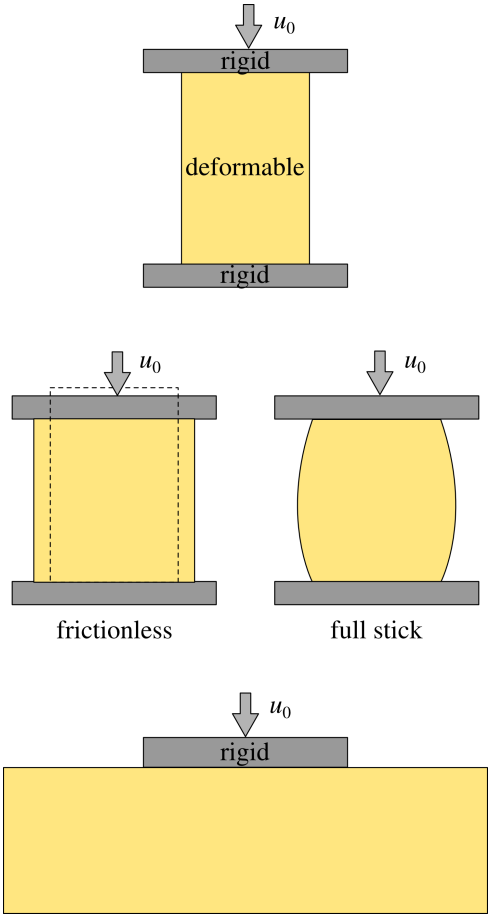

Figure 1.11: Flat geometry: comparison between frictionless, full stick, and rigid indenter boundary conditions.

This condition simply means that in persisting contact the point can only move tangentially to the surface. In finite element software, this kind of conditions coupling degrees of freedom is called *multi-point constraints* or MPC.

1.8.1 General classification of boundary conditions

In classical contact problems we can combine different boundary conditions in special ways in order to represent different contact scenarios. These boundary-conditions combinations can be classified as follows:

Type I: prescribed tractions (Neumann)

$$p(x,y), \quad \tau_x(x,y), \quad \tau_y(x,y). \tag{1.88}$$

Type II: prescribed displacements (Dirichlet)

$$\underline{\boldsymbol{u}}(x,y). \tag{1.89}$$

This full Dirichlet problem represents sticking contact with infinite friction.

Type III: mixed boundary conditions Normal displacement and tangential tractions, or vice versa:

$$u_z(x,y), \quad \tau_x(x,y), \quad \tau_y(x,y), \tag{1.90}$$

or

$$p(x,y), \quad u_x(x,y), \quad u_y(x,y). \tag{1.91}$$

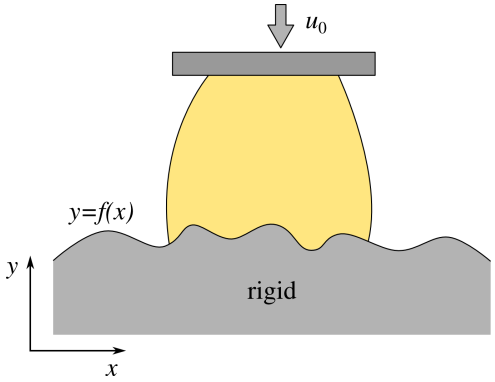

Figure 1.12: Curved rigid surface: the contact constraint becomes a geometric condition in the current configuration.

Type IV: displacement with traction relation (nonlinear) Displacement is prescribed in the normal direction, while tangential tractions satisfy a constitutive relation:

$$u_z(x, y), \qquad \tau_x(x, y) = \pm f\, p(x, y). \tag{1.92}$$

This combination makes sense for frictional contact in full slip state, when we know the contact pressure and assume that the shear traction is simply $\tau_x = fp$, $\tau_y = 0$ for sliding along OX direction.

1.9 Basics of Friction

1.9.1 Existence of frictional resistance.

The existence of frictional resistance is experimentally evident. A tangential force is required to initiate sliding between two bodies in contact. Moreover, classical experiments show that the critical tangential force does not depend on the nominal contact area, but primarily on the normal load.

Historical experiments. Early quantitative observations of friction are attributed to Leonardo da Vinci, whose notebook drawings documented two fundamental facts: the proportionality between frictional force and weight, and the independence of friction from the apparent contact area, see Figure 1.13.

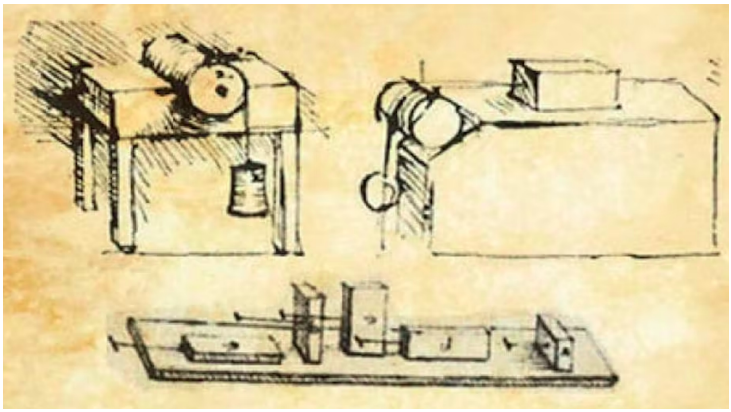

Figure 1.13: Leonardo da Vinci's early friction experiments.

1.9.2 Global description.

Consider a rigid block on a flat surface subjected to a normal force N and a tangential force T, see Figure 1.14. Two regimes are observed:

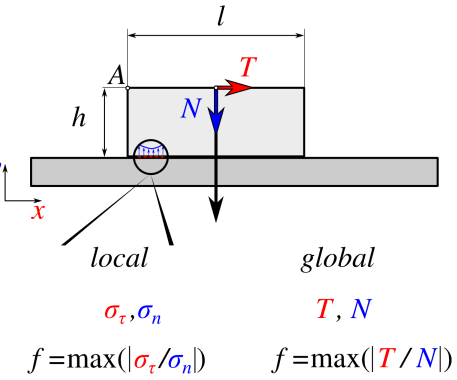

Figure 1.14: Rectangle on a flat surface subjected to normal and tangential loads: the macroscopic friction f_{glob} can be determined by measuring the maximal tangential load T for a given normal load N and taking their ratio. On the mesoscopic scale, the local f_{loc} is governed by microscopic pressure and shear. On an even smaller scale, a shear threshold τ_c exists at microscopic asperity contacts.

$$T < T_c(N) \quad \text{stick}, \tag{1.93}$$

$$T = T_c(N) \quad \text{slip}. \tag{1.94}$$

Experiments show that the critical force is proportional to the normal load,

$$T_c \sim N. \tag{1.95}$$

This motivates the definition of the global friction coefficient

$$f = \left| \frac{T_c}{N} \right|. \tag{1.96}$$

1.9.3 Mesoscopic description.

At the local (mesoscopic) level, friction is expressed in terms of tractions. Let

$$\boldsymbol{\sigma} \cdot \underline{\boldsymbol{n}} = \underline{\boldsymbol{t}}$$

denote the surface traction. Its normal component is

$$\sigma_n = (\boldsymbol{\sigma} \cdot \underline{\boldsymbol{n}}) \cdot \underline{\boldsymbol{n}},$$

and the tangential traction reads

$$\underline{\boldsymbol{\sigma}}_t = \boldsymbol{\sigma} \cdot \underline{\boldsymbol{n}} - \sigma_n \underline{\boldsymbol{n}}.$$

The local stick and slip conditions become

$$\|\underline{\boldsymbol{\sigma}}_t\| < \tau_c(\sigma_n) \quad \text{stick}, \tag{1.97}$$

$$\|\underline{\boldsymbol{\sigma}}_t\| = f|\sigma_n| \quad \text{slip}. \tag{1.98}$$

The statistical properties of the local and global friction could differ significantly but the mean value should coincide within the quasistatic conditions.

1.9.4 Microscopic description.

The underlying mechanism may be interpreted in terms of interfacial adhesion. At the microscopic scale, the interface sustains a finite shear strength. We therefore introduce a threshold shear traction τ_c at the interface and assume that for a local shear below this threshold no sliding occurs.

Consider a contact interface subject to compressive force N acting over a nominal surface A_0, resulting in nominal pressure $p_0 = N/A_0$. We know that all surfaces are rough (see **??**) and because of this roughness,

the true contact area denoted A is generally smaller than the nominal contact area A_0. At the same time, at moderate loads, the contact area increases approximately proportionally to the pressure

$$\frac{A}{A_0} = bp_0 = bN/A_0 \quad \Rightarrow \quad A = bN$$

where b is the proportionality factor. Then if at every contact area, the threshold shear resistance is given by τ_c, then the macroscopic slip starts only when all contact points in the contact interface reach this threshold. By integrating over the surface we obtain the maximal tangential force that the surface can sustain

$$T_{\max} = \int_S \tau_c dS = A\tau_c = \tau_c bN.$$

Here the product $\tau_c b$ is interpreted as a coefficient of friction. This theory is called *adhesive theory of friction*. Here, however, we demonstrated a very simplistic explication of friction. A more detailed analysis will be carried out in **??**.

⚠ Friction is Not Conservative

In the absence of friction, contact is a conservative problem. The solution follows from an energy minimization principle subject to unilateral constraints. The final configuration depends only on the current loading and not on the loading history. With friction, the problem becomes *path-dependent*. The current state depends on the entire loading history, starting from the first contact. Therefore, frictional problem cannot be formulated as a minimization problem. In practice, one have to carefully model the whole history in order to capture the correct solution.

Example. Spring on frictional substrate.

Regardless its ubiquity, it is a complex phenomenon even in the simples mathematical model and our frictional intuition sometimes is not very reliable. To demonstrate this complexity we will solve a frictional problem of a spring with one degree of freedom.

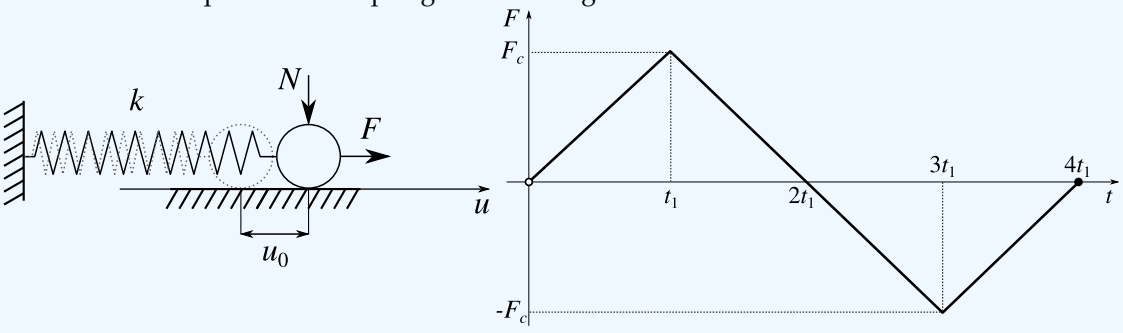

Set-up Consider a one degree-of-freedom frictional system depicted in the figure above. Spring's stiffness is k, externally applied force $F(t)$ changes in time, normal force N remains constant, u denotes the location of the contact point along OU axis. The contact interface is governed by Coulomb's law with the friction coefficient f. The spring is stretched by displacement u_0 from its equilibrium state $u = 0$ and is brought in frictional contact by normal force N. Note that after removing the displacement control the point remains in stick conditions. The external forcing changes F with time. Inertial effects are neglected.

Task How does the position of the contact point u changes if the external load is applied according to the following law (see the figure above):

$$F(t) = \begin{cases} F_c t/t_1, & 0 \le t < t_1 \\ F_c(2t_1 - t)/t_1, & t_1 \le t < 3t_1 \\ F_c(t - 4t_1)/t_1, & 3t_1 \le t < 4t_1 \end{cases}$$

In two words it corresponds to the load F monotonically increasing from zero to F_c, then monotonically decreasing to $-F_c$, and finally monotonically increasing again to 0. Since the spring is linearly elastic (rate independent) as well as the friction law, the rate at which the force changes do not alter the solution.

Solution

- The frictional force F_t is bounded by a product of the friction coefficient f and the absolute value of the normal force $|N|$:
$$|F_f| \le f|N|$$
In the *stick state*, the frictional force can point either in left or right direction in order to equilibrate other forces acting in the system to ensure that the contact point does not move $\dot{u} = 0$. In the *slip state*, the frictional force is opposite to the direction of relative motion[a]
$$\text{sign}(F_f) = -\text{sign}(\dot{u}),$$
where
$$\text{sign}(x) = \begin{cases} 1, & x > 0; \\ 0, & x = 0; \\ -1, & x < 0. \end{cases}$$
The absolute value of the frictional force is equivalent to $f|N|$.

- Since according to the problem set-up, in the beginning (at $t = 0$) the mass sticks to the ground we can deduce that the reaction force in the spring $F_s = -ku_0$ (produced by the initial displacement u_0) could be equilibrated by the frictional force $F_s + F_f = 0$. Therefore, since the frictional force is bounded by $|F_f| \le f|N|$, then the initial displacement is also bounded:
$$k|u_0| \le f|N| \quad \Leftrightarrow \quad -f|N|/k \le u_0 \le f|N|/k.$$

- For increasing external force $F \sim t$, before the frictional force reaches its limit, the system will remain in stick condition $u = u_0$, the equilibrium of forces can be written as follows:
$$-ku_0 + F_f + F = 0 \quad \Leftrightarrow \quad -ku_0 + F_f + F_c t/t_1 = 0,$$
the frictional force adjusts itself to ensure the equilibrium, i.e.
$$F_f = ku_0 - F_c t/t_1.$$

- When frictional force reaches its limit[b], i.e.
$$F_f = -f|N| = ku_0 - F_c t/t_1,$$
which happens at time
$$t_r = (ku_0 + f|N|)t_1/F_c,$$

then the contact point will start to move in the right direction following the increasing force F. The corresponding external force at $t = t_r$ is given by

$$F_r = ku_0 + f|N|$$

If however, $t_r < t_1$ no slip will start up to the moment when external force reaches its maximum value. Later, when the external force inverses its sign ($t > 2t_1$) the stick state will be preserved up to the minimal value $F = -F_c$ if $|-ku_0 - F_c| < f|N|$, otherwise the point will start to slip to the left.

- Let us assume that $t_r < t_1$ and the point starts to slip before the external force reaches its maximum value. Then the increasing external force can no longer be balanced by frictional force (which remains constant in slip), but will be balanced by the reaction force in the spring that will stretch more. Since the spring is linear, it will stretch proportionally to the difference between the external force and the frictional force:

  $$k\Delta u = F_c(t - t_r)/t_1$$

  The force equilibrium can be written as:

  $$-k\,[u_0 + \Delta u] - f|N| + F_c t/t_1 = 0$$

- At reaching $t = t_1$ (corresponding to the maximal external force), the force equilibrium takes the following form:

  $$-k\,[u_0 + \Delta u^*] - f|N| + F_c = 0 \qquad (*)$$

  from which the total slip can be found

  $$\Delta u^* = (F_c - f|N|)/k - u_0.$$

- When the external force inverses at $t = t_1$ and start to decrease to zero in the interval $t_1 \le t \le 2t_1$, three scenarios can be considered:

  1. **Scenario 1**: Mass-point continues to move to the right.
  2. **Scenario 2**: Mass-point moves to the left.
  3. **Scenario 3**: Mass-point sticks to the current location and does not move.

  To choose the *only possible* scenario, let us denote by δu the point displacement increment from its location found at $t = t_1$, by δt we denote the time increment $\delta t = t - t_1$, by $-\delta F < 0$ we denote the external force increment which is negative and is given by $-F_c\delta t/t_1$; finally, δF_f will denote the increment of the frictional force. We can rewrite (*) at $t = t_1 + \delta t$ as follows:

  $$-k\,[u_0 + \Delta u^* + \delta u] - f|N| + \delta F_f + F_c - \delta F = 0$$

  by subtracting (*) from this equation we obtain:

  $$-k\delta u + \delta F_f - \delta F = 0. \qquad (**).$$

  Scenario 1 assumes that $\delta u > 0$, then from (**) it follows that the frictional force increment takes the form:

  $$\delta F_f = \delta F + k\delta u > 0.$$

  Then the total frictional force is given by $F_f = -f|N| + \delta F_f$. It means that its absolute value becomes less than the frictional limit $|F_f| < f|N|$. However, in this case the point should switch to the stick state, since in slip, the frictional force should be at its extreme value.

However, since we assumed in this scenario that the point continues its motion to the right, we obtain a contradiction. So this scenario is impossible.

Scenario 2 assumes that $\delta u < 0$, then (**) is given by

$$-k\delta u + \delta F_f - \delta F = 0.$$

At the same time, to let the point move to the right the frictional force should take the value $f|N|$ and should be directed to the right (opposite to the point motion), i.e. $\delta F_f = 2|f|N$. But it is unphysical that frictional force switches abruptly. Consider, for example, a box that we move forward with a force F, it slides smoothly at constant velocity v. Now, imagine that we slightly decreased the force $F - \delta F$, and the box slipped immediately back, because the frictional force which opposed the motion switched the sign. It does not happen. Such an abrupt switch would also imply that the following equation is satisfied:

$$-k\delta u + 2|f|N - \delta F = 0,$$

which has no solution for small time and displacement increments, i.e. for both $\delta t \to 0$ and $\delta u \to 0$. To satisfy this equation the point mass should jump to the left by

$$\delta u = (2|f|N - \delta F)/k.$$

Hence, if the frictional force is allowed to switch abruptly, the equilibrium cannot be ensured for arbitrary external force history. All this is unphysical and thus Scenario 2 must be excluded.

Scenario 3 assumes that $\delta u = 0$, then (**) transforms into

$$\delta F_f - \delta F = 0, \qquad (***)$$

which implies that frictional force increment balances the external force increment. The total frictional force is $F_f = -f|N| + \delta F$, and its absolute value is below the frictional limit $|F_f| < f|N|$, thus the point should remain in stick, and it is what was assumed in this scenario. So no contradiction is found here, no abrupt changes in forces happen, and equilibrium can be satisfied at each time moment. So Scenario 3 is the only possible.

- At time t_l such that $t_1 < t_l \leq 3t_1$, the frictional force increment will reach its maximum value $\delta F_f = 2f|N|$, i.e. the total frictional force will point to the right and be equal by value $f|N|$. To find t_l, we replace the external force increment δF by $F_c \delta t/t_1$ and obtain the following equation:

$$2f|N| = F_c \delta t/t_1,$$

which gives

$$\delta t = 2f|N|t_1/F_c,$$

so the total time of the start of backward motion is given by

$$t_l = t_1 + \delta t = t_1\left[1 + \frac{2f|N|}{F_c}\right]. \qquad (\star)$$

The resulting force is given by:

$$F_l = F_c - 2f|N|.$$

If the initial position $u_0 > 0$, then it can be shown that $f|N| < F_c$ and thus the inversion of motion will always happen before $t = 3t_1$, since the square brackets in ($\star$) is bounded as

$$1 \leq \left[1 + \frac{2f|N|}{F_c}\right] \leq 3.$$

For $t_l \leq t \leq 3t_1$ the point will slip to the left and squeeze the spring which will balance the excess of the external force.

- At time $t > t_3$ the point will stick again and retain its position until $t = 4t_1$.

Graphically, the solution is depicted in the figure below. The easiest way to solve this problem geometrically is to plot the solution in force-displacement coordinates as in the figure below(a). Two parallel lines of slope $1/k$, symmetric over $F = 0$ and spaced by $2f|N|$ mark lines on which the slip will happen. In between them, the stick zone is located. The initial stick zone is coloured in light green: any pair of force and displacement will result in stick state. On the left line, the motion can occur only to the left, on the right line, it can occur only in the right direction, in between no motion is possible. The resulting solution in displacement-time coordinates is given in the figure below(b).

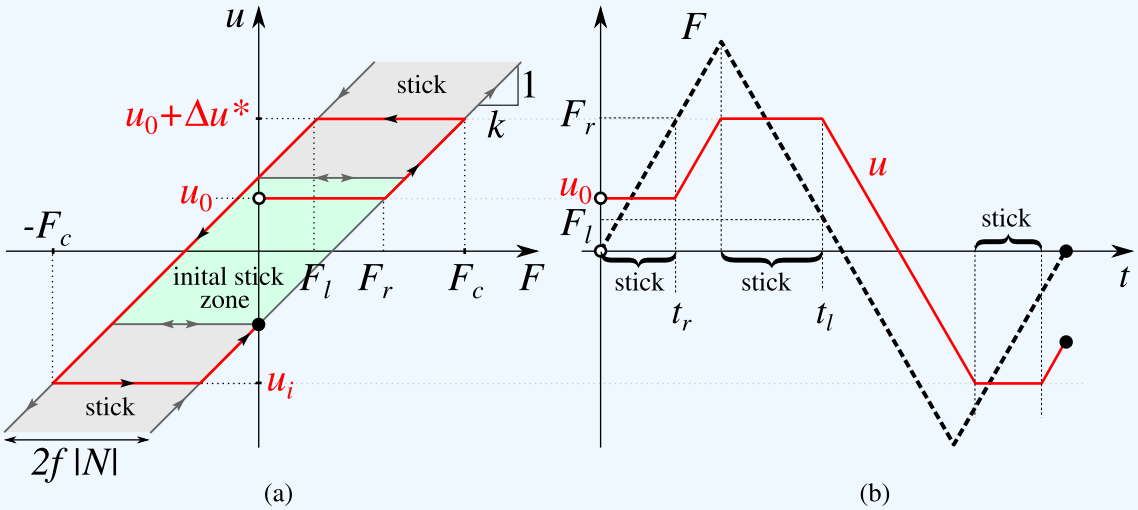

Solution of the problem: (a) solution in force-displacement space, initial stick zone is coloured in light green; (b) force and displacement are depicted as functions of time.

[a] Since we assume that the rigid flat ground does not move nor deform, the relative motion reduces to the absolute motion of the mass point.

[b] We take the frictional force with the negative sign since when the point starts to slip to the right, the frictional force should point to the left.

1.10 Direction of Sliding

Sliding on an inclined plane. Consider a block resting on an inclined plane. The gravitational acceleration is vertical, while the plane is tilted. The block does not move, i.e. the frictional force compensate for the tangent component of the weight $T_w = mg\tan(\alpha)$ directed in the tangent plane in the direction OY. Suppose a tangential force $\underline{\boldsymbol{T}}_f = T_f \underline{\boldsymbol{e}}_x$ is imposed orthogonally to the slope direction, see Figure 1.15. Then the total force acting on the block is a sum of both $T = \sqrt{T_f^2 + T_w^2}$. When the value of this tangential force reach the frictional threshold $\mu mg\arctan(\alpha)$ the sliding will start. Since the frictional force is exactly opposes the sliding velocity, the sliding will start not along the OX direction not straight down the slope, but somewhere in between.

1.11 Relative sliding velocity

Relative sliding between a slave point and a deformable master surface. Let us return to our master slave representation. The kinematics of frictional contact requires a precise definition of the *relative sliding velocity* between a slave point and the master surface. The master Γ_m surface is parametrized by

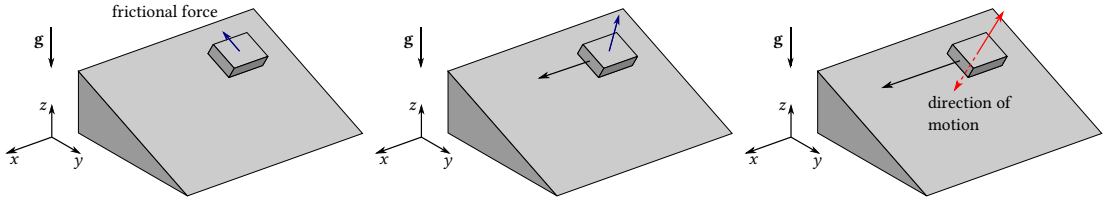

Figure 1.15: A block on an inclined plane $z = -ay$ is pulled by a force applied parallel to OX direction, the frictional force increases and gradually changes when the pulling force increses and when reaching the frictional limit an oblique sliding initiates with the sliding velocity and frictional resistance opposing each other.

convective coordinates $\xi_i, \qquad i = 1, 2$

$$\forall \underline{\boldsymbol{x}}(\xi_1, \xi_2) \in \Gamma_m.$$

If the surface is smooth, we can define a tangent plane at every point of the surface passing through two tangent vectors

$$\underline{\boldsymbol{\tau}}_1 = \frac{\partial \underline{\boldsymbol{x}}}{\partial \xi_1}, \quad \underline{\boldsymbol{\tau}}_2 = \frac{\partial \underline{\boldsymbol{x}}}{\partial \xi_2}.$$

Let $\underline{\boldsymbol{r}}_s(t)$ denote the position of the slave point and $\underline{\boldsymbol{x}}(\xi_{*1}(t), \xi_{*2}(t), t)$ its projection on the master surface. The relative tangent velocity on the deforming master surface is given by

$$\underline{\boldsymbol{v}}_t = \frac{\partial \underline{\boldsymbol{\rho}}}{\partial \xi_1}\dot{\xi}_1 + \frac{\partial \underline{\boldsymbol{\rho}}}{\partial \xi_2}\dot{\xi}_2 = \tau_i \dot{\xi}_i \tag{1.99}$$

which expresses it as a linear combination of the local tangent basis. This derivative does not represent a time derivative of any particular vector but it is a so-called Lie derivative with respect to evolving vector field. It could be thought as *fisherman analogy* (see Figure 1.17 or **??**): when you are in a boat brought by ocean currents, you move with respect to the solid earth surface but are immobile with respect to the surrounding water, i.e. your relative motion with respect to the water is zero. But if you switch on the boat's engine, you will move with respect to the solid earth and also with respect to the water around.

Figure 1.16 schematically illustrates the motion of a slave point sliding over a deforming master surface. The projection point moves because of both surface deformation and evolution of the convective coordinates. The resulting tangential gap g_t evolves accordingly.

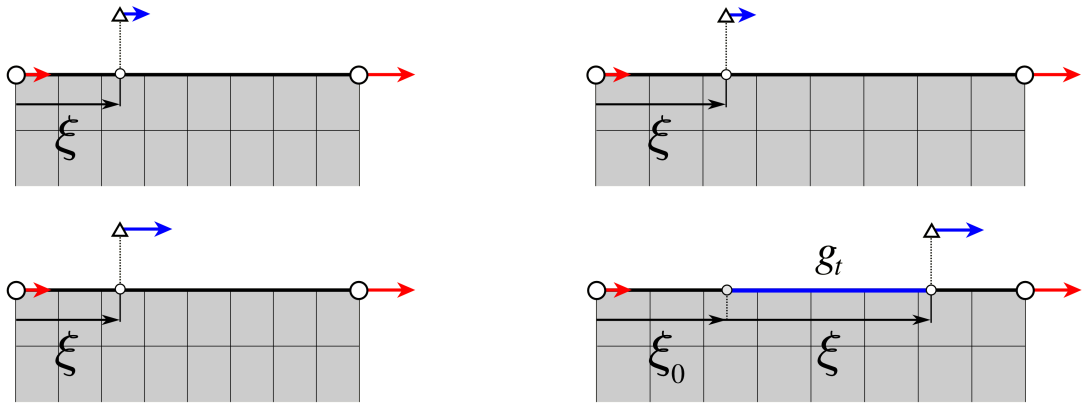

Figure 1.16: Relative slip between a slave point and a deformable master surface: *upper panel*: left – initial configuration, right – next configuration: no relative sliding occurs $|\underline{\boldsymbol{v}}_t| = 0$, *lower panel*: left – initial configuration, right – next configuration: the slave point slides with respect to the deforming master surface $|\underline{\boldsymbol{v}}_t| > 0$.

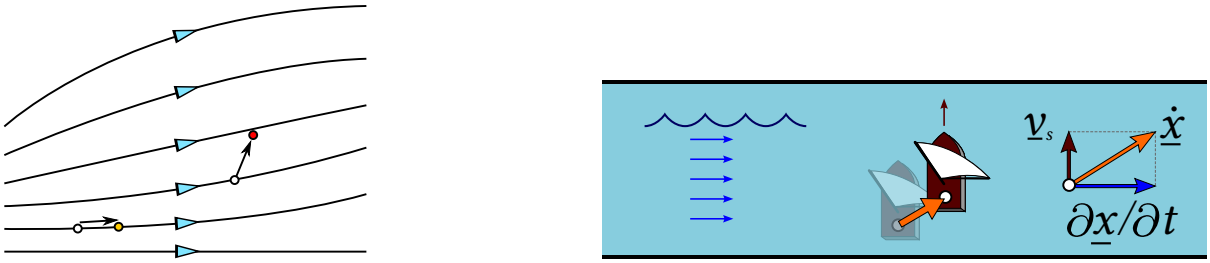

(a) (b)

Figure 1.17: This sketch shows Fisherman's analogy: (a) observing the flow relative to the boat motivates the decomposition into "motion at fixed coordinates" and "motion due to coordinate drift", i.e. a Lie-derivative viewpoint: the change of a vector field along the change of another vector field; (b) - a similar sketch of a boat crossing a river, the sliding velocity with respect to the river is giveb by $\underline{v}_s = \dot{x} - \partial \underline{x}/\partial t$.

Example. Relative sliding velocity.

Relative sliding in one dimension. A simple one-dimensional setting clarifies how the tangential relative motion arises from the evolution of the convective coordinate. Consider a segment BC in the current configuration, and a point A whose projection on BC is P, see **??**. Let $\xi \in [0,1]$ be the convective coordinate of P along the segment, so that

$$x_P(\xi, t) = \xi\, x_C(t) + (1-\xi)\, x_B(t). \tag{1.100}$$

The velocity of the projection point follows from the chain rule,

$$\dot{x}_P = \frac{d}{dt} x_P(\xi(t), t) = \underbrace{\frac{\partial x_P}{\partial t}}_{\text{motion at fixed } \xi} + \underbrace{\frac{\partial x_P}{\partial \xi}\,\dot{\xi}}_{\text{motion along the segment}}. \tag{1.101}$$

Using (1.100), these terms are

$$\frac{\partial x_P}{\partial t} = \xi\,\dot{x}_C + (1-\xi)\,\dot{x}_B, \qquad \frac{\partial x_P}{\partial \xi} = x_C - x_B. \tag{1.102}$$

The tangential slip velocity is defined as the part of $\dot{x}_P$ associated with the change of the convective coordinate, i.e. the difference between the total velocity and the velocity at fixed ξ:

$$v_t = \dot{x}_P - \frac{\partial x_P}{\partial t} = \frac{\partial x_P}{\partial \xi}\,\dot{\xi} = (x_C - x_B)\,\dot{\xi} = \frac{\partial x}{\partial \xi}\,\dot{\xi}. \tag{1.103}$$

Over a time step $t^n \to t^{n+1}$, the corresponding tangential slip increment can be approximated by freezing the tangent at ξ^n:

$$\Delta g_t^{n+1} \approx \left.\frac{\partial x}{\partial \xi}\right|_{\xi^n} (\xi^{n+1} - \xi^n). \tag{1.104}$$

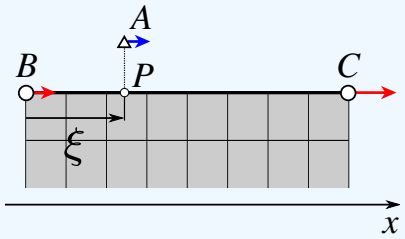

One-dimensional relative slip: the projection point P moves because of both the motion of the segment BC and the evolution of the convective coordinate ξ.

1.12 Frictional Constraints: Amontons–Coulomb Friction Law

Frictional states: stick and slip. Define the friction function (like a yield function in plasticity)

$$f(\underline{\sigma}_t, \sigma_n) = |\underline{\sigma}_t| - \mu|\sigma_n|. \tag{1.105}$$

The admissible set of tangential tractions corresponds to

$$f \le 0, \tag{1.106}$$

which corresponds geometrically to the interior of the Coulomb cone in stress space, see Figure 1.19–Figure 1.18. If $f < 0$, then the point is in *sticking state* and its relative sliding velocity should be zero $\underline{v}_t = 0$. The frictional force can take any value such that $|\underline{\sigma}_t| < \mu|\sigma_n|$, i.e. the point in space $\{\sigma_{t1}, \sigma_{t2}, |\underline{v}_t|\}$ is

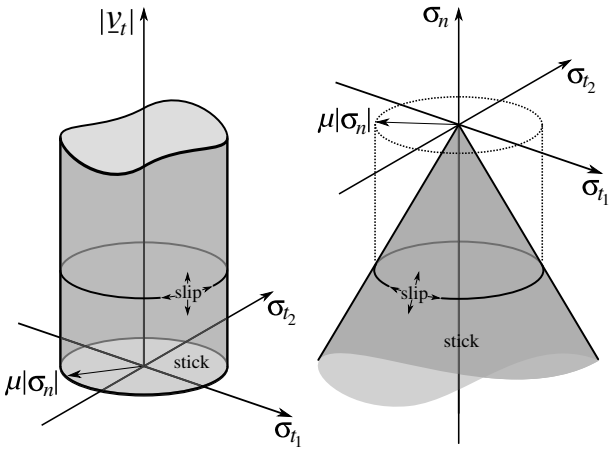

Figure 1.18: (Left) frictional tractions and kinetics: space $\{\sigma_{t1}, \sigma_{t2}, |\underline{v}_t|\}$: the sticking points can be only located in the basement circular region; in the sliding state, the points are located at the surface of the cylinder. (Right) link between tangential and normal tractions are represented by Coulomb's cone in three dimensions: space $\{\sigma_{t1}, \sigma_{t2}, \sigma_n\}$: sticking points are inside the code, sliding points are on its surface.

located within the base circle locate at $|\underline{v}_t| = 0$ (see Figure 1.18 - left) and in space $\{\sigma_{t1}, \sigma_{t2}, \sigma_n\}$ the point is located within the Coulomb's cone (see Figure 1.18 - right). If $f = 0$, the point is in *sliding state* and is located on the slip surface and can slide under the action of frictional resistance $\underline{\sigma}_t$ such that $|\underline{\sigma}_t| = \mu|\sigma_n|$. In space $\{\sigma_{t1}, \sigma_{t2}, |\underline{v}_t|\}$, the sliding point is located on the surface of the cylinder (see Figure 1.18 - left) and in space $\{\sigma_{t1}, \sigma_{t2}, \sigma_n\}$ it is located on the surface of the Coulomb's cone (see Figure 1.18 - right). Note that the frictional resistance opposes the sliding direction:

$$\frac{\underline{v}_t}{|\underline{v}_t} = -\frac{\underline{\sigma}_t}{|\underline{\sigma}_t|}$$

In 2D, a simpler illustration of frictional sliding can be drawn

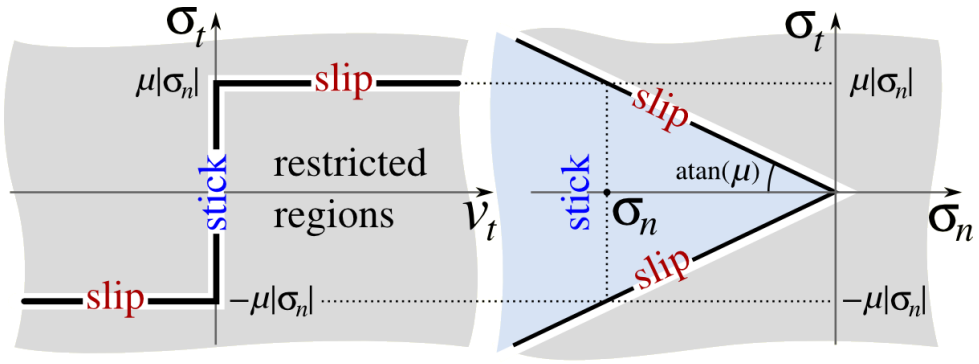

Figure 1.19: Illustration of a link between frictional traction σ_t, sliding velocity v_t and contact normal traction σ_n in two-dimensional case.

Contact states. Frictional contact combines normal unilateral constraints with a tangential frictional condition. Contrary to the normal contact exhibiting only two states (contact or no-contact), in frictional case, we distinguish three states:

- **No contact.**

$$g > 0, \qquad \sigma_n = 0. \tag{1.107}$$

- **Sticking contact**

$$|\underline{v}_t| = 0, \qquad f < 0. \tag{1.108}$$

- **Sliding contact**

$$|\underline{v}_t| > 0, \qquad f = 0. \tag{1.109}$$

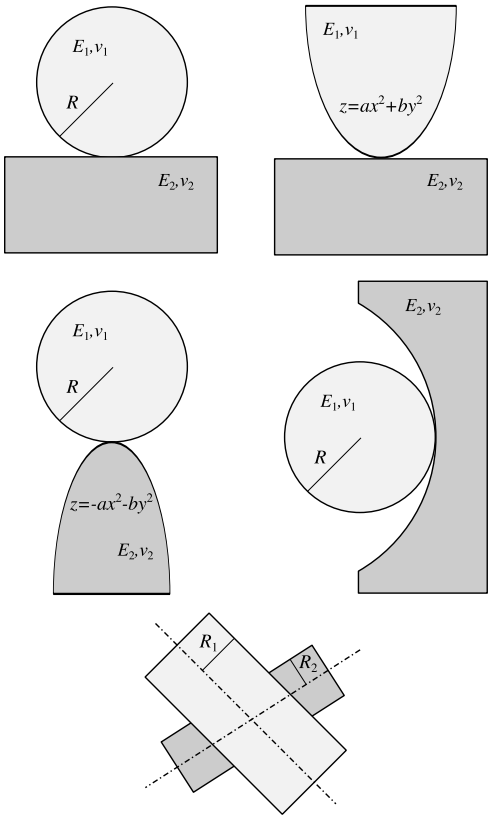

Figure 1.20: Different configurations which can be solved using Hertz theory.

Complementarity structure. Stick and slip are mutually exclusive. This is expressed by the complementarity condition

$$|\underline{v}_t|\left(|\underline{\sigma}_t| - \mu|\sigma_n|\right) = 0, \tag{1.110}$$

together with

$$|\underline{v}_t| \geq 0, \qquad |\underline{\sigma}_t| - \mu|\sigma_n| \leq 0. \tag{1.111}$$

This structure is analogous to the Hertz-Signorini-Moreau conditions in the normal direction and corresponds to a KKT-type system. These equations, have to be complemented by the sliding direction conditions resulting in the following set of conditions:

$$\boxed{|\underline{v}_t| \geq 0, \quad |\underline{\sigma}_t| - \mu|\sigma_n| \leq 0, \quad |\underline{v}_t|\left(|\underline{\sigma}_t| - \mu|\sigma_n|\right) = 0, \quad \frac{\underline{\sigma}_t}{|\underline{\sigma}_t|} = -\frac{\underline{v}_t}{|\underline{v}_t|}} \tag{1.112}$$

1.13 Hertzian Contact

Hertzian contact is one of the most elegant and widely used analytical solutions in solid mechanics. As stated by Kenneth L. Johnson from University of Cambridge and the author of a famous book on contact mechanics (Johnson 1987), *"His theory, worked out during the Christmas vacation 1880 at the age of 23(!), aroused considerable interest . . . "*. It beautifully combines two geometries and two different elastic materials in a small set of relevant parameters and derives 3-4 elegant equations linking indentation (or approach), force and contact radius - the three key components in every contact problem. In practice, a very broad class of contact problems can be reduced to Hertzian contact, at least in the first approximation (see Figure 1.20)

Assumptions. Hertzian contact describes the frictionless, non-adhesive contact between two elastic bodies under the following assumptions:

- Linear isotropic elasticity;
- Small strains;
- Smooth surfaces which can be locally described by a quadratic form;
- No friction and no adhesion;
- Contact region small compared to radii of curvature - it excludes conformal contact.

The statement that surfaces can be locally approximated by quadratic forms implies the following representation:

$$z_i(x,y) = z_i^0 + \tfrac{1}{2}X^\top K_i X, \quad K_i = \begin{bmatrix} K_i^{11} & K_i^{12} \\ K_i^{12} & K_i^{22} \end{bmatrix}, \quad X = \begin{bmatrix} x \\ y \end{bmatrix}.$$

In coordinates corresponding to principal curvatures κ_x, κ_y, the curvature matrix K is diagonal:

$$K = \begin{bmatrix} \kappa_1 & 0 \\ 0 & \kappa_2 \end{bmatrix}$$

In the general case, the surfaces of contacting surfaces are not necessarily aligned, and therefore the gap can be represented as

$$g(x,y) = z_2(x,y) - z_1(x,y) = g_0(x,y) + \tfrac{1}{2}X^\top(K_2 - K_1)X. \tag{1.113}$$

We can, however, always select axes x', y' for which the resulting curvature matrix $K = K_2 - K_2$ is diagonal, then

$$g(x',y') = z_2(x',y') - z_1(x',y') = g_0(x',y') + \tfrac{1}{2}\kappa_1^* x^2 + \kappa_2^* y^2. \tag{1.114}$$

Note that principal effective curvatures κ_1^* and κ_2^* can be of different sign. The link between curvatures and curvature radii is simply $R_i^* = 1/\kappa_i^*$. The star notation denotes that these values combine information of both contacting solids.

Let us consider several classical configurations:

- **Solids of revolution**: $\kappa_1^* = \kappa_2^*$ and the gap can be described in polar coordinates

  $$g(r) = g_0(r) + \frac{r^2}{2R^*},$$

  the effective curvature radius can be seen as a combination of two curvature radius of two contacting solids of revolution

  $$\frac{1}{R^*} = \frac{1}{R_1} + \frac{1}{R_2}. \tag{1.115}$$

  Example 1: if one solid is flat $R_1 \to \infty$ then the effective curvature is simply the curvature of another solid $R^* = R_2$.
  Example 2: if two similar parabolic surface of curvature radous $R_1 = R_2 = R$ come in contact, the total curvature is given by $R^* = R/2$.

- **Line contact**: if $\kappa_1^* = 0$ (equivalently $R_1^* \to \infty$), we are in situation of line contact, for example between cylinders. As before, the effective curvature is then by Equation (1.115).

- **Slight ellipticity:** if κ_1^* and κ_2^* do not differ very much a good approximation could be obtained if one replaces this contact by a contact of revolution with the effective curvature $\kappa = \sqrt{\kappa_1^* \kappa_2^*}$ (Johnson 1987; Greenwood 2006).

Effective elastic modulus. When studying Boussinesq solution, one can observe that for a given pressure distribution $p(x, y)$ the vertical displacement scales as

$$u_z^i \sim \frac{1-\nu_i^2}{E_i} p(x,y), \quad i \in \{1,2\}.$$

Since in the contact, the pressure induced at on both contacting surfaces is the same but just opposite in direction, the total gap will be changed as

$$g(x,y) = g_0(x,y) + u_z^1 - u_z^2 = g_0(x,y) + \frac{1}{\pi}\left(\frac{1-\nu_1^2}{E_1} + \frac{1-\nu_2^2}{E_2}\right)\int_S G(x-x', y-y')p(x',y')\,dS,$$

where $G(x-x', y-y')$ is the Green kernel. This implies that one can simply formulate the contact problem for an effective or combined elastic modulus E^*

$$\frac{1}{E^*} = \frac{1-\nu_1^2}{E_1} + \frac{1-\nu_2^2}{E_2}. \tag{1.116}$$

1.13.1 Axisymmetric (3D) contact.

For axisymmetric contact of effective radius R^* between elastic solids with the composite elastic modulus E^* subject to normal force F, the contact region is circular of radius a. The displacement parameter δ represents the approach between distant points in two solids at the instance of the first touch. Then according to Hertz solution, the link between approach and the contact radius is given by

$$\boxed{\delta = \frac{a^2}{R^*}} \quad \Leftrightarrow \quad \boxed{a = \sqrt{\delta R^*}} \tag{1.117}$$

The contact pressure distribution reads

$$\boxed{p(r) = p_0\sqrt{1-\frac{r^2}{a^2}},} \qquad 0 \le r < a, \quad p_0 = \frac{3F}{2\pi a^2}. \tag{1.118}$$

The pressure vanishes abruptly at the edge (the slope is infinite) with the asymptotics $p \sim \sqrt{a-r}$.

The total force is

$$F = \int_0^a 2\pi r p(r)\,dr = \frac{2}{3}\pi a^2 p_0. \tag{1.119}$$

Eliminating p_0 gives the classical relations

$$\boxed{a = \left(\frac{3FR^*}{4E^*}\right)^{1/3}} \tag{1.120}$$

and the force-indentation law

$$\boxed{F = \frac{4}{3}E^*\sqrt{R^*}\,\delta^{3/2}} \tag{1.121}$$

1.13.2 Line contact (cylinders)

For two parallel cylinders (plane strain), the contact region is a strip of half-width a. The contact pressure is the same:

$$\boxed{p(x) = p_0\sqrt{1-\frac{x^2}{a^2}},} \qquad 0 \le x < a. \tag{1.122}$$

But other relations become

$$p_0 = \frac{2F}{\pi a}. \tag{1.123}$$

$$\boxed{a = \left(\frac{4FR^*}{\pi E^*}\right)^{1/2}}, \tag{1.124}$$

In contrast to the axisymmetric case, the approach δ does not appear in the key equations because of the logarithmic nature of vertical displacement which depend on the datum.

1.14 Sinusoidal Contact

1.15 Rolling Contact

1.16 Other Classical Contact Problems and Reading

Analytical solutions in continuum mechanics are in general difficult to obtain, especially in three-dimensional cases. Adding such a non-linear ingredient as contact, makes them even more difficult. Adding friction on the top makes them almost impossible to solve. The difficulties include (1) complex geometries which cannot be resolved within Hertz theory, (2) finite friction or adhesion, (3) impossibility to use homogeneous half-space approximation, for example in case of finite thickness or coatings, (4) need for capturing anisotropic or non-linear material behavior, (5) elasto-hydrolubrication regime requires simultaneous solution for both elastic and thin flow problems. Nevertheless, there is plenty of analytical solutions which could be helpful at least to construct an approximate quantitative understanding for more complex problems. A non-exhaustive list of such problems is given below:

- Various problems with rigid flat stamps:
  circular, elliptic, frictionless, full-stick, finite friction.
- Wedges *(coin)* and cones in elasticity and plasticity.
- Circular inclusion in a conforming hole
  Steuermann, 1939, Goodman, Keer, 1965
- Frictional indentation $z \sim x^n$
  Incremental approach Mossakovski, 1954
  self-similar solution Spence, 1968, 1975
- Adhesive contact Johnson et al, 1971, 1976
- Contact with layered materials (coatings)
- Elastic-plastic and viscoelastic materials
- Sliding/rolling of non-conforming bodies
  Cattaneo (1938), Mindlin (1949), Galin (1953), Goryacheva (1998)
  Note: $u_r \sim (1-2\nu)/G$, so if $(1-2\nu_1)/G_1 = (1-2\nu_2)/G_2$ tangential tractions do not change normal ones

Bibliography

Aragón, Alejandro M, Vladislav A Yastrebov, and Jean-François Molinari (2013). "A constrained-optimization methodology for the detection phase in contact mechanics simulations". In: *International Journal for Numerical Methods in Engineering* 96.5, pp. 323–338.

Greenwood, JA2295174 (2006). "A simplified elliptic model of rough surface contact". In: *Wear* 261.2, pp. 191–200.

Johnson, Kenneth Langstreth (1987). *Contact mechanics*. Cambridge: Cambridge university press.

Yastrebov, Vladislav A (2013). *Numerical methods in contact mechanics*. John Wiley & Sons.